Accepted Manuscript

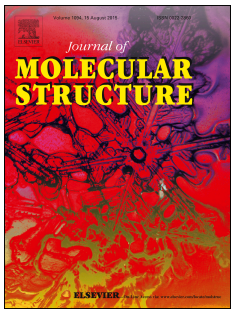

Synthesis, structure characterization, *in vitro* and *in silico* biological evaluation of a new series of thiazole nucleus integrated with pyrazoline scaffolds

Rajitha Sadashiva, Damodara Naral, Jyothi Kudva, S. Madan Kumar, K. Byrappa, R. Mohammed Shafeeulla, Manjunatha Kumsi

PII: S0022-2860(17)30678-6

DOI: 10.1016/j.molstruc.2017.05.066

Reference: MOLSTR 23807

To appear in: *Journal of Molecular Structure*

Received Date: 13 March 2017

Revised Date: 15 May 2017

Accepted Date: 15 May 2017

Please cite this article as: R. Sadashiva, D. Naral, J. Kudva, S. Madan Kumar, K. Byrappa, R. Mohammed Shafeeulla, M. Kumsi, Synthesis, structure characterization, *in vitro* and *in silico* biological evaluation of a new series of thiazole nucleus integrated with pyrazoline scaffolds, *Journal of Molecular Structure* (2017), doi: 10.1016/j.molstruc.2017.05.066.

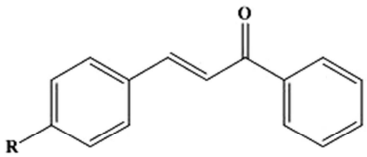

Chalcone derivatives

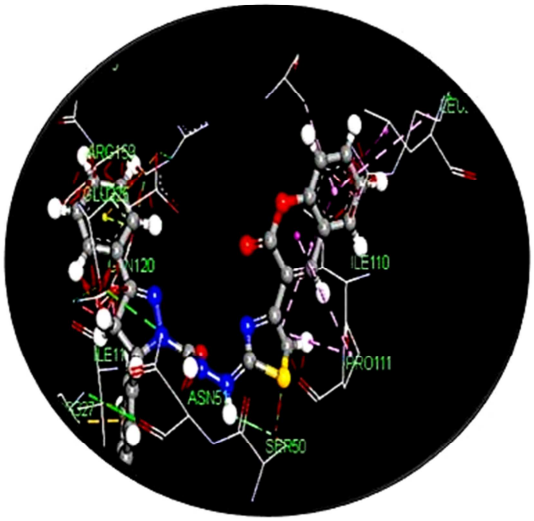

Docking study

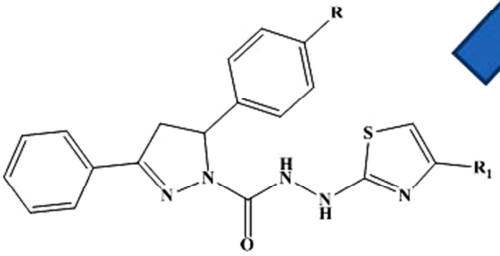

Thiazole nucleus integrated with pyrazoline scaffolds

Synthesis, structure characterization, *in vitro* and *in silico* biological evaluation of a new series of thiazole nucleus integrated with pyrazoline scaffolds

Rajitha Sadashiva[a], Damodara Naral[b], Jyothi Kudva[c*], S. Madan Kumar[d], Byrappa K[e], Mohammed Shafeeulla R[f], Manjunatha Kumsi[g].

[a]Sigma-Aldrich Chemical Pvt. Ltd., Bommasandra-Jigani link Road, Bengaluru, 560100, INDIA.
[b]Department of Chemistry, Canara Engineering College, Benjanapadavu, Mangaluru, 574219, INDIA.
[c*]Department of Chemistry, St Joseph Engineering College, Vamanjoor, Mangaluru, 575005, INDIA.
[d]DST-PURSE Lab., Mangalagangotri, Mangalore University, Mangaluru, 574199, INDIA.
[e]Department of Materials Science, Mangalagangotri, Mangalore University, Mangaluru, 574199, INDIA.
[f]Department of Chemistry, Sahyadri Science College, Shimoga, 577 201, INDIA.
[g]Department of Chemistry, Nagarjuna College of Engineering and Technology, Bengalure, 562164, INDIA.

Keywords: Thiazole, Anticancer activity, Molecular docking, Single crystal XRD.

ABSTRACT

In the current study, a series of 2,4-disubstituted-1,3-thiazoles linked with pyrazoline scaffolds **3a-o** were rationally designed and synthesized. The structures of the title compounds were elucidated by spectroscopic data (UV-Vis, IR, NMR and Mass spectra) and elemental analysis. Single crystal X-Ray diffraction studies revealed that, the compounds **3i** and **3k** crystallized in monoclinic crystal system with $P2_1/n$ space group and Z = 4. The molecules **3i** and **3k** were connected with intermolecular hydrogen bonds N2—H2...O1, N3---H3...Cl1 and short contacts (C---H... π and C---Cl...π). Intramolecular hydrogen bonds, N3---H3...N5 and C5----H5....N1 were also existed. The compounds were evaluated for their anticancer activity against A549 and MCF-7 human cancer cell lines and *in vitro* antimicrobial activity against pathogenic microbial strains. The compounds bearing chloro atom at the *para* position of phenyl ring A like **3f**, **3j** and **3k** with the IC_{50}: 7.5, 5.0 and 5.0 µM respectively, exhibited better activity than standard drug Cisplatin (IC_{50}: 10.0 µM). In addition, the compounds **3a**, **3f**, **3j** and **3l** have exhibited the similar antimicrobial activity as that of standard drug Ciprofloxacin and Fluconazole. Furthermore, to support the biological potency of the compounds, *in silico* molecular docking studies were carried out against the *E. coli* MurB (PDB code: 2MBR) and Jnk1 inhibitor (PDB code: 3v3v) enzymes. The various types of interactions between the compounds and amino acid residue of enzymes were also reported.

1. Introduction

The global burden of cancer continues to increase largely because of aging and growth of the population. Cancers figure among the leading causes of morbidity and mortality worldwide and the cancer report 2016 by WHO states that, with approximately 14 million new cases and 8.2 million cancer-related deaths in 2012. The number of new cases is expected to rise by about 70% over the next 2 decades. Cancer is the second most common cause of death in the US, exceeded only by heart disease and accounts for nearly 1 of every 4 deaths [1]. The development of new anticancer agents is becoming the major interest in many academic and industrial research laboratories all over the world, with the aim to develop more potent molecules with higher specificity and reduced toxicity.

During the research for an effective anticancer drug, some of the pharmacologically active heterocyclic compounds having thiazole moiety were found to have good anticancer potency [2-4]. The active heterocyclic ring thiazole was found in many potent biologically active molecules, such as Sulfathiazole (antimicrobial drug), Ritonavir (antiretroviral drug), Abafungin (antifungal drug). The activity capacity of thiazole nucleus depended on the substitution pattern at thiazole ring [5]. The applications of thiazoles were found in drug development for the treatment of allergies [6], hypertension [7], inflammation [8], schizophrenia [9], bacterial [10], HIV infections [11] and hypnotics [12]. In addition to above fact, the thiazole derivatives having pyrazoline moiety have exhibited the anticancer [13] and antimicrobial activity [14-16].

E. coli MurB enzyme is essential for the viability of bacterial cells [17,18] and it is an attractive target for inhibitors with the potential to have broad antibacterial activity. The enzymes involved in peptidoglycan biosynthesis are among the best-known targets in the search for new antibiotics [19]. The JNKs are master protein kinases that regulate many physiological processes, including inflammatory responses, morphogenesis, cell proliferation, differentiation, survival and death. It is increasingly apparent that, persistent activation of JNKs is involved in cancer development and progression. Therefore, JNKs represent attractive targets for therapeutic intervention with small molecule kinase inhibitors [20,21].

X-ray crystallography is the most comprehensive technique available to determine the structure of any molecule at atomic resolution. Results from X-ray crystallographic studies provide unambiguous, accurate and reliable 3-dimensional structural parameters at times even before complete chemical characterization is available. The X-ray diffraction data is also useful to determine the ferroelectric property of the solid structure [22-27].

In the view of the wide potential applications of thiazole and pyrazoline derivatives, synthesis of a new series of 1,3-thiazoles integrated pyrazoline scaffolds **3a-o** were undertaken. The structures of the newly synthesized molecules were assigned on the basis of a detailed study on UV-Vis, FTIR, ^{1}H NMR, ^{13}C NMR, mass and elemental analysis. The lattice parameters, bond lengths, bond angles, dihedral angles, torsion angles, hydrogen bonding and intermolecular interactions of the compounds **3i** and **3k** were obtained from single crystal X-ray diffraction technique. The molecules were screened for their anticancer potency against the A549 and MCF-7 human cancer cell lines. The molecules were tested for the antimicrobial property against *Staphylococcus aureus* MTCC 96, *Bacillus subtilis* MTCC 441, *Pseudomonas aeruginosa* MTCC 1688, *Escherichia coli* MTCC 443, *Aspergillus niger* MTCC 282 and *Candida albicans* MTCC 227. The activity data was supported by the molecular docking studies. The standard drugs, Ciprofloxacin and Cisplatin were docked against *E. coli* MurB and Jnk1 inhibitor enzymes, respectively.

2. Experimental

2.1. Chemistry

All the reactions were carried out in oven-dried glassware and under the nitrogen atmosphere. The chemicals used for reaction were from Sigma-Aldrich Chemical Pvt. Ltd. Bengaluru, India. Melting points were determined in open capillary tube on BUCHI melting point M-565 apparatus and were uncorrected. The homogeneity, follow up of the reaction and purity of the compounds were checked by thin layer chromatography recoated silica gel $60F_{254}$ plates. 10% methanol in chloroform was used as mobile phase and spots were detected by their absorption under UV light. The elemental and spectral analysis was carried out in analytical lab, Sigma-Aldrich Chemical Pvt. Ltd. Bengaluru, India. Elemental analysis was performed on Leco-932 CHNS analyser. The UV-Vis spectra of the compounds were determined using Perkin-Elemer lambda spectrometer and methanol was used as a solvent. IR spectra were recorded in Perkin Elmer FTIR 100 series spectrometer. Samples were dried at 100^{0}C and 16 scans were averaged across the spectral range of 4000-600 cm^{-1}. The IR stretching frequencies of the important functional groups were reported in cm^{-1}. The NMR

spectra were recorded in DMSO-d_6 at ambient temperature using Bruker amx 400 spectrometer operating at 400 MHz and 100 MHz for ^{1}H and ^{13}C nuclei, respectively. The mass spectra of compounds were recorded on Agilent LC/MVD XCT plus mass spectrometer.

*2.1.1. Synthesis of 1,3-thiazoles integrated pyrazoline derivatives (**3a-o**).*

The 3-(4-substitutedphenyl)-1-phenylprop-2-en-1-one (chalcones) derivatives **1a-e** were synthesized by using the procedure mentioned in the literature [28]. Typically, various phenyl aldehyde (0.1mol) and acetophenone (0.1mol) were coupled in presence of 10% KOH in ethanol. 1, 3, 5-trisubstituted pyrazoline ring was constructed using the suitable chalcone and carbazide in methanol [29]. The products were characterized by ^{1}HNMR spectra.

The hydrazinecarbothioamide derivative of pyrazolines (**2a-e)** was obtained by treating the carbohydrazide derivative of pyrazolines with potassium thiocyanate and hydrochloric acid in water [30]. The products were characterized by ^{1}HNMR spectra.

A mixture of a suitable hydrazinecarbothioamide derivative of pyrazolines (**2a-e**) (0.1mol), 2-bromo-1-substitutedethan-1-one (0.1mol) and sodium acetate (0.2 mol) in 10 ml of ethanol was refluxed for 4 h. The progress of the reaction was monitored using thin layer chromatography. After completion of the reaction, on cooling the solid product obtained was collected by filtration and purified by recrystallisation from dimethyl formamide to give pure desired title compounds with good yields. After drying the samples at 100^{0}C, physical properties, overall yields and spectral data of the compounds were noted.

*2.1.2. 5-(4-chlorophenyl)-3-phenyl-N'-(4-phenyl-1,3-thiazol-2-yl)-4,5-dihydro-1H -pyrazole-1-carbohydrazide (**3a**).*

Yield, 80 %; light yellow solid; m.p. 205-207 ^{0}C. UV-Vis λ_{max} (nm): 290.07, 224.69. IR (cm^{-1}): 3399 (N-H), 3296 (N-H), 3048 (C-Harom), 1659 (C=O), 1596 (C=N), 1516 (C=N). ^{1}H NMR (DMSO-d_6) δ (ppm): 3.13 (dd, 1H, C$\underline{H}_a$H, *J* = 5.6 Hz, 18.0 Hz), 3.76 (dd, 1H, CH$\underline{H}_b$, *J* = 12.0 Hz, 18.4 Hz), 5.45 (dd, 1H, C$\underline{H}_c$, *J* = 5.2 Hz, 12.8 Hz), 6.78 (s, 1H, C$\underline{H}^t$), 7.14 (m, 2H, aromatic), 7.20 (m, 3H, aromatic), 7.27 (t, 2H, aromatic, *J* = 7.4 Hz), 7.39 (m, 3H, aromatic), 7.67 (m, 3H, aromatic), 9.31 (s, 1H, N$\underline{H}^{2N}$), 9.60 (s, 1H, N$\underline{H}^{1N}$). ^{13}C NMR (DMSO-d_6) δ (ppm): 41.56, 59.32, 103.19, 125.15, 125.73, 126.22, 126.75, 127.55, 127.93, 127.95, 128.22, 129.76, 132.78, 133.87, 139.23, 151.2, 152.41, 153.10, 172.38. ESI MS: m/z = 474.1 $[M+H]^+$. Anal. Calcd. for $C_{25}H_{20}ClN_5OS$: C, 63.35; H, 4.25; N, 14.78; S, 6.76, found: C, 63.33; H, 4.21; N, 14.70; S, 6.80.

*2.1.3. 5-(4-bromophenyl)-3-phenyl-N'-(4-phenyl-1,3-thiazol-2-yl)-4,5-dihydro-1H -pyrazole-1-carbohydrazide (**3b**).*

Yield, 82%; brown solid; m.p. 210-212 ^{0}C. UV-Vis λ_{max} (nm): 290.10, 225.14. IR (cm^{-1}): 3398 (N-H), 3297 (N-H), 1661 (C=O), 1594 (C=N), 1517 (C=N). ^{1}H NMR (DMSO-d_6) δ (ppm): 3.14 (dd, 1H, C$\underline{H}_a$H, *J* = 6.0 Hz, 18.0Hz), 3.86 (dd, 1H, CH$\underline{H}_b$, *J* = 12.0 Hz, 17.8 Hz), 5.51 (dd, 1H, C$\underline{H}_c$, *J* = 5.0 Hz, 12.0 Hz), 7.20 (m, 2H, aromatic), 7.22 (s, 1H, C$\underline{H}^t$), 7.27 (t, 1H, aromatic, *J* = 7.13 Hz,), 7.38 (t, 2H, aromatic, *J* = 7.62 Hz), 7.46 (t, 3H, aromatic, *J* = 8.31 Hz), 7.51 (m, 2H, aromatic m), 7.81 (m, 2H, aromatic), 7.89 (m, 2H, aromatic), 9.39 (s, 1H, N$\underline{H}^{2N}$), 9.67 (s, 1H, N$\underline{H}^{1N}$). ^{13}C NMR (DMSO-d_6) δ (ppm): 41.55, 59.99, 102.71, 120.71, 125.49, 126.82, 127.36, 127.84, 128.48, 130.05, 131.12, 131.44, 134.79, 142.18, 150.58, 152.22, 153.87, 173.69. ESI MS: m/z = 520.1 $[M+H]^+$. Anal. Calcd. for $C_{25}H_{20}BrN_5OS$: C, 57.92; H, 3.89; N, 13.51; S, 6.18, found: C, 57.91; H, 3.91; N, 13.48; S, 6.19.

*2.1.4. 5-(4-methylphenyl)-3-phenyl-N'-(4-phenyl-1,3-thiazol-2-yl)-4,5-dihydro-1H-pyrazole-1-carbohydrazide (**3c**).*

Yield, 78%; white solid; m.p. 200-202 ^{0}C. UV-Vis λ_{max} (nm): 290.52, 223.80. IR (cm^{-1}): 3414 (N-H), 3182 (N-H), 1672 (C=O), 1598 (C=N), 1504 (C=N). ^{1}H NMR (DMSO-d_6) δ (ppm): 2.25 (s, 3H, C$\underline{H}_3$), 3.10 (dd, 1H, C$\underline{H}_a$H, *J* = 5.2 Hz, 17.9 Hz), 3.84 (dd, 1H, CH$\underline{H}_b$, *J* = 11.8 Hz, 17.86 Hz), 5.45 (dd, 1H, C$\underline{H}_c$, *J* = 5.17 Hz, 11.94 Hz), 7.11 (m, 4H, aromatic), 7.20

(s, 1H, C$\underline{H}^{t}$), 7.27 (t, 1H, aromatic, *J* = 7.36 Hz), 7.38 (t, 2H, aromatic, *J* = 7.39 Hz), 7.46 (m, 3H, aromatic), 7.81 (m, 2H, aromatic), 7.88 (m, 2H, aromatic), 9.37 (s, 1H, N$\underline{H}^{2N}$), 9.63 (s, 1H, N$\underline{H}^{1N}$). ^{13}C NMR (DMSO-d_6) δ (ppm): 20.65, 41.92, 60.22, 102.76, 125.39, 125.50, 126.74, 127.35, 128.49, 128.61, 129.05, 129.96, 131.27, 134.82, 136.27, 139.87, 150.62, 152.12, 153.88, 173.83. ESI MS: m/z = 454.2 $[M+H]^+$. Anal. Calcd. for $C_{26}H_{23}N_5OS$: C, 68.85; H, 5.11; N, 15.44; S, 7.07, found: C, 68.80; H, 5.13; N, 15.50; S, 7.10.

*2.1.5. 5-(4-methoxyphenyl)-3-phenyl-N'-(4-phenyl-1,3-thiazol-2-yl)-4,5-dihydro-1H -pyrazole-1-carbohydrazide (**3d**).*

Yield, 80%; white powder; m.p. 212-214 ^{0}C. UV-Vis λ_{max} (nm): 290.96, 227.36. IR (cm^{-1}): 3382 (N-H), 3304 (N-H), 1668 (C=O), 1595 (C=N), 1509 (C=N). ^{1}H NMR (DMSO-d_6) δ (ppm): 3.11 (dd, 1H, C$\underline{H}_a$H, *J* = 5.52 Hz, 17.18 Hz), 3.70 (s, 3H, OC$\underline{H}_3$), 3.83 (dd, 1H, CH$\underline{H}_b$, *J* = 11.96 Hz, 18.85 Hz), 5.44 (dd, 1H, C$\underline{H}_c$, *J* = 5.0 Hz, 12.0 Hz), 6.86 (m, 2H, aromatic), 7.16 (m, 2H, aromatic), 7.19 (s, 1H, C$\underline{H}^{t}$), 7.27 (t, 1H, aromatic, *J* = 7.12 Hz), 7.38 (t, 2H, aromatic, *J* = 7.56 Hz), 7.45 (m, 3H, aromatic), 7.81 (m, 2H, aromatic), 7.89 (m, 2H, aromatic), 9.36 (s, 1H, N$\underline{H}^{2N}$), 9.60 (s, 1H, N$\underline{H}^{1N}$). ^{13}C NMR (DMSO-d_6) δ (ppm): 41.80, 55.05, 60.01, 102.72, 113.91, 125.51, 126.76, 127.00, 127.33, 128.49, 128.60, 129.94, 131.32, 134.81, 132.01, 150.59, 152.13, 153.83, 158.46, 173.90. ESI MS: m/z = 470.2 $[M+H]^+$. Anal. Calcd. for $C_{26}H_{23}N_5O_2S$: C, 66.51; H, 4.94; N, 14.91; S, 6.83, found: C, 66.55; H, 4.90; N, 14.95; S, 6.80.

*2.1.6. 5-(4-methoxyphenyl)-N'-[4-(naphthalen-2-yl)-1,3-thiazol-2-yl]-3-phenyl-4,5 -dihydro-1H-pyrazole-1-carbohydrazide (**3e**).*

Yield, 75%; Tan powder; m.p. 194-196 ^{0}C. UV-Vis λ_{max} (nm): 297.93, 235.37. IR (cm^{-1}): 3402 (N-H), 3181 (N-H), 1680 (C=O), 1593 (C=N), 1500 (C=N). ^{1}H NMR (DMSO-d_6) δ (ppm): 3.14 (dd, 1H, C$\underline{H}_a$H, *J* = 5.0 Hz, 17.9 Hz), 3.67 (s, 3H, OC$\underline{H}_3$), 3.84 (dd, 1H, CH$\underline{H}_b$, *J* = 12.0 Hz, 18.0 Hz), 5.46 (dd, 1H, C$\underline{H}_c$, *J* = 5.0 Hz, 11.0Hz), 6.86 (m, 2H, aromatic), 7.17 (m, 2H, aromatic), 7.35 (s, 1H, C$\underline{H}^{t}$), 7.46 (m, 5H, aromatic), 7.91 (m, 6H, aromatic), 7.92 (m, 6H, aromatic), 8.35 (s, 1H, aromatic), 9.16 (s, 1H, N$\underline{H}^{2N}$), 9.63 (s, 1H, N$\underline{H}^{1N}$). ^{13}C NMR (DMSO-d_6) δ (ppm): 41.81, 55.05, 60.02, 103.66, 113.88, 123.99, 125.89, 126.38, 126.79, 127.52, 128.03, 128.59, 129.95, 131.31, 1321.24, 133.14, 134.81, 150.43, 152.13, 153.88, 158.40, 173.83. ESI MS: m/z = 520.2 $[M+H]^+$. Anal. Calcd. for $C_{30}H_{25}N_5O_2S$: C, 69.34; H, 4.85; N, 13.48; S, 6.17, found: C, 69.38; H, 4.89; N, 13.50; S, 6.20.

*2.1.7. 5-(4-chlorophenyl)-N'-[4-(naphthalen-2-yl)-1,3-thiazol-2-yl]-3-phenyl-4,5 -dihydro-1H-pyrazole-1-carbohydrazide (**3f**).*

Yield, 68%; light yellow powder; m.p. 204-206 ^{0}C. UV-Vis λ_{max} (nm): 296.74, 237.59. IR (cm^{-1}): 3386 (N-H), 3174 (N-H), 1685 (C=O), 1591 (C=N), 1503 (C=N). ^{1}H NMR (DMSO-d_6) δ (ppm): 3.16 (dd, 1H, C$\underline{H}_a$H, *J* = 5.6 Hz, 18.0 Hz), 3.88 (dd, 1H, CH$\underline{H}_b$ *J* = 12.4 Hz, 18.0 Hz), 5.52 (dd, 1H, C$\underline{H}_c$, *J* = 5.2 Hz, 12.0 Hz), 7.29 (m, 2H, aromatic), 7.37 (m, 2H, aromatic), 7.4 (s, 1H, C$\underline{H}^{t}$), 7.48 (m, 5H, aromatic), 7.90 (m, 6H, aromatic), 8.34 (s, 1H, aromatic), 9.43 (d, 1H, N$\underline{H}^{2N}$), 9.71 (d, 1H, N$\underline{H}^{1N}$). ^{13}C NMR (DMSO-d_6) δ (ppm): 41.67, 60.04, 103.64, 123.98, 125.88, 126.37, 126.83, 127.57, 127.79, 128.01, 128.52, 128.63, 130.07, 131.15, 131.72, 132.27, 133.15, 141.76, 150.56, 152.33, 153.91, 174.00. ESI MS: m/z = 524.2 $[M+H]^+$. Anal. Calcd. for $C_{29}H_{22}ClN_5OS$: C, 66.47; H, 4.23; N, 13.36; S, 6.12, found: C, 66.40; H, 4.28; N, 13.30; S, 6.15.

*2.1.8. 5-(4-methoxyphenyl)-N'-[4-(4-methylphenyl)-1,3-thiazol-2-yl]-3-phenyl-4,5-dihydro -1H-pyrazole-1-carbohydrazide (**3g**).*

Yield, 68%; light brown powder; m.p. 202-204 ^{0}C. UV-Vis λ_{max} (nm): 290.07, 228.25. IR (cm^{-1}): 3433 (N-H), 3192 (N-H), 1685 (C=O), 1558 (C=N), 1504 (C=N). ^{1}H NMR (DMSO-d_6) δ (ppm): 2.30 (s, 3H, C$\underline{H}_3$), 3.10 (dd, 1H, C$\underline{H}_a$H, *J* = 5.2 Hz, 18.52 Hz), 3.70 (s, 3H, OC$\underline{H}_3$), 3.82 (dd, 1H, CH$\underline{H}_b$, *J* = 12.24 Hz, 17.62 Hz), 5.44 (dd, 1H, C$\underline{H}_c$ *J* = 4.8 Hz, 12.01 Hz), 6.86 (d, 2H, aromatic, *J* = 7.89 Hz), 7.10 (s, 1H, C$\underline{H}^{t}$), 7.12 (m, 4H, aromatic),

7.61 (m, 3H, aromatic), 7.70 (m, 2H, aromatic), 7.85 (m, 2H, aromatic), 9.31 (s, 1H, N$\underline{H}^{2N}$), 9.58 (s, 1H, N$\underline{H}^{1N}$). ^{13}C NMR (DMSO-d_6) δ (ppm): 20.83, 41.89, 55.10, 60.03, 101.91, 113.84, 125.45, 126.76, 128.60, 129.06, 129.95, 131.28, 132.16, 134.82, 136.59, 150.61, 152.13, 153.84, 158.38, 173.6. ESI MS: m/z = 484.2 $[M+H]^+$. Anal. Calcd. for $C_{27}H_{25}N_5OS$: C, 67.06; H, 5.21; N, 14.48; S, 6.63, found: C, 67.10; H, 5.28; N, 14.50; S, 6.66.

*2.1.9. 5-(4-methylphenyl)-N'-[4-(naphthalen-2-yl)-1,3-thiazol-2-yl]-3-phenyl-4,5 -dihydro-1H-pyrazole-1-carbohydrazide (**3h**).*

Yield, 75%; white powder; m.p. 206-208 ^{0}C. UV-Vis λ_{max} (nm): 296.74, 237.14. IR (cm^{-1}): 3391 (N-H), 3183 (N-H), 1685 (C=O), 1593 (C=N), 1501 (C=N). ^{1}H NMR (DMSO-d_6) δ (ppm): 2.24 (s, 3H, C$\underline{H}_3$), 3.11 (dd, 1H, C$\underline{H}_a$H, *J* = 5.0 Hz, 18.0 Hz), 3.85 (dd, 1H, CH$\underline{H}_b$, *J* = 12.0 Hz, 18.5 Hz), 5.46 (dd, 1H, C$\underline{H}_c$, *J* = 5.0 Hz, 12.0 Hz), 7.12 (m, 4H, aromatic), 7.36 (s, 1H, C$\underline{H}^t$), 7.46 (m, 5H, aromatic), 7.92 (m, 6H, aromatic), 8.34 (s, 1H, aromatic), 9.42 (s, 1H, N$\underline{H}^{2N}$), 9.67 (s, 1H, N$\underline{H}^{1N}$). ^{13}C NMR (DMSO-d_6) δ (ppm): 20.65, 41.89, 60.15, 103.62, 123.93, 124.02, 125.42, 125.88, 126.37, 126.78, 127.52, 128.06, 128.61, 129.07, 129,99, 131.29, 132.30, 133.14, 136.29, 139.87, 150.61, 152.20, 153.89, 174.04. ESI MS: m/z = 504.2 $[M+H]^+$. Anal. Calcd. for $C_{30}H_{25}N_5OS$: C, 71.55; H, 5.00; N, 13.91; S, 6.37, found: C, 71.60; H, 5.02; N, 13.95; S, 6.40.

*2.1.10. N'-[4-(4-chlorophenyl)-1,3-thiazol-2-yl]-5-(4-methylphenyl)-3-phenyl-4,5 -dihydro-1H-pyrazole-1-carbohydrazide (**3i**).*

Yield, 75%; white powder; m.p. 244-246 ^{0}C. UV-Vis λ_{max} (nm): 292.74, 230.03. IR (cm^{-1}): 3411 (N-H), 3182 (N-H), 1678 (C=O), 1594 (C=N), 1501 (C=N). ^{1}H NMR (DMSO-d_6) δ (ppm): 2.25 (s, 3H, C$\underline{H}_3$), 3.10 (dd, 1H, C$\underline{H}_a$H, *J* = 4.8 Hz, 17.6 Hz), 3.84 (dd, 1H, CH$\underline{H}_b$, *J* = 12.0 Hz, 18.5 Hz), 5.45 (dd, 1H, C$\underline{H}_c$, *J* = 5.2 Hz, 12.0 Hz), 7.11 (m, 4H, aromatic), 7.26 (s, 1H, C$\underline{H}^t$), 7.44 (m, 5H, aromatic), 7.83 (m, 2H, aromatic), 7.88 (m, 2H, aromatic), 9.40 (s, 1H, N$\underline{H}^{2N}$), 9.63(s, 1H, N$\underline{H}^{1N}$). ^{13}C NMR (DMSO-d_6) δ (ppm): 20.67, 41.85, 60.29, 103.51, 125.44, 126.77, 127.18, 128.50, 128.59, 129.05, 129.96, 131.24, 131.74, 133.65, 136.27, 139.85, 149.27, 152.20, 153.77, 173.95. ESI MS: m/z = 489.2 $[M+H]^+$. Anal. Calcd. for $C_{26}H_{22}ClN_5OS$: C, 63.99; H, 4.45; N, 14.35; S, 6.57, found: C, 63.90; H, 4.48; N, 14.30; S, 6.60.

*2.1.11. 5-(4-chlorophenyl)-N'-[4-(2-oxo-3,8a-dihydro-2H-1-benzopyran-3-yl)-1,3 -thiazol-2-yl]-3-phenyl-4,5-dihydro-1H-pyrazole-1-carbohydrazide (**3j**).*

Yield, 70%; white crystals; m.p. 230-232 ^{0}C. UV-Vis λ_{max} (nm): 356.34, 291.41. IR (cm^{-1}): 3437 (N-H), 3164 (N-H), 1718 (C=O), 1689 (C=O), 1607 (C=N), 1504 (C=N). ^{1}H NMR (DMSO-d_6) δ (ppm): 3.16 (dd, 1H, C$\underline{H}_a$H, *J* = 5.65 Hz, 18.0 Hz), 3.88 (dd, 1H, CH$\underline{H}_b$, *J* = 12.45 Hz, 17.45 Hz), 5.50 (dd, 1H, C$\underline{H}_c$, *J* = 5.36 Hz, 11.91 Hz), 7.27 (d, 2H, aromatic, *J* = 8.7 Hz), 7.43 (m, 7H, aromatic), 7.62 (m, 1H, aromatic), 7.66 (s, 1H, C$\underline{H}^t$), 7.85 (dd, 1H, aromatic, *J* = 1.38 Hz, *J* = 7.97 Hz), 7.89 (m, 2H, aromatic), 8.53 (s, 1H, aromatic), 9.49 (s, 1H, N$\underline{H}^{2N}$), 9.76 (s, 1H, N$\underline{H}^{1N}$). ^{13}C NMR (DMSO-d_6) δ (ppm): 41.72, 60.03, 109.77, 115.85, 119.19, 120.43, 124.71, 126.83, 127.58, 128.53, 128.61, 128.77, 130.09, 131.10, 131.62, 131.73, 138,19, 141.65, 143.85, 152.23, 152.40, 153.78, 158.70, 173.35. ESI MS: m/z = 542.1 $[M+H]^+$. Anal. Calcd. for $C_{28}H_{22}ClN_5O_3S$: C, 61.82; H, 4.08; N, 12.87; S, 5.89, found: C, 61.80; H, 4.10; N, 12.90; S, 5.86.

*2.1.12. 5-(4-chlorophenyl)-N'-[4-(4-chlorophenyl)-1,3-thiazol-2-yl]-3-phenyl-4,5 -dihydro-1H-pyrazole-1-carbohydrazide (**3k**).*

Yield, 73%; white solid; m.p. 227-229 ^{0}C. UV-Vis λ_{max} (nm): 291.41, 225.14. IR (cm^{-1}): 3409 (N-H), 3129 (N-H), 2650 (C-Harom), 1698 (C=O), 1616 (C=N), 1504 (C=N). ^{1}H NMR (DMSO-d_6) δ (ppm): 3.14 (dd, 1H, C$\underline{H}_a$H, *J* = 5.60 Hz, 17.41 Hz), 3.84 (dd, 1H, CH$\underline{H}_b$, *J* = 12.03 Hz, 18.13 Hz), 5.49 (dd, 1H, C$\underline{H}_c$, *J* = 5.43 Hz, 11.37 Hz), 7.24 (s, 1H, C$\underline{H}^t$), 7.26 (m, 2H, aromatic), 7.38 (m, 2H, aromatic), 7.44 (m, 5H, aromatic), 7.81 (d, 2H, aromatic, *J* = 8.61 Hz), 7.88 (m, 2H, aromatic), 9.46 (s, 1H,

N<u>H</u>^{2N}), 9.69 (s, 1H, N<u>H</u>^{1N}). ^{13}C NMR (DMSO-d_6) δ (ppm): 41.83, 60.06, 103.84, 126.80, 127.26, 127.56, 128.52, 128.54, 128.60, 130.09, 131.08, 131.72, 131.97, 133.14, 141.66, 148.52, 152.40, 153.73, 173.94. ESI MS: m/z = 508.1 $[M+H]^+$. Anal. Calcd. for $C_{25}H_{19}Cl_2N_5OS$: C, 59.06; H, 3.77; N, 13.78; S, 6.31, found: C, 59.10; H, 3.70; N, 13.80; S, 6.28.

*2.1.13. 5-(4-chlorophenyl)-N'-[4-(4-methylphenyl)-1,3-thiazol-2-yl]-3-phenyl-4,5 -dihydro-1H-pyrazole-1-carbohydrazide (**3l**).*

Yield, 68%; light brown solid; m.p. 199-201 ^{0}C. UV-Vis λ_{max} (nm): 289.63, 223.80. IR (cm^{-1}): 3437 (N-H), 3191 (N-H), 1685 (C=O), 1598 (C=N), 1505 (C=N). ^{1}H NMR (DMSO-d_6) δ (ppm): 2.36 (s, 3H, C<u>H</u>$_3$), 3.20 (dd, 1H, C<u>H</u>$_a$H, *J* = 5.56 Hz, 17.88 Hz), 3.93 (dd, 1H, CH<u>H</u>$_b$, *J* = 12.05 Hz, 18.36 Hz), 5.56 (dd, 1H, , C<u>H</u>$_c$, *J* = 5.36 Hz, 12.00 Hz), 7.17 (s, 1H, C<u>H</u>^{t}), 7.24 (d, 2H, aromatic, *J* = 8.06 Hz), 7.32 (d, 2H, aromatic, *J* = 8.32 Hz), 7.44 (d, 2H, aromatic, *J* = 8.83 Hz), 7.5 (m, 3H, aromatic), 7.75 (d, 2H, aromatic, *J* = 8.09 Hz), 7.94 (m, 2H, aromatic), 9.39 (s, 1H, N<u>H</u>^{2N}), 9.71(s, 1H, N<u>H</u>^{1N}). ^{13}C NMR (DMSO-d_6) δ (ppm): 20.81, 41.62, 59.89, 101.84, 125.46, 126.79, 127.53, 128.52, 129.06, 130.01, 131.15, 131.70, 132.18, 136.58, 141.74, 150.65, 152.26, 153.93, 173.63. ESI MS: m/z = 488.2 $[M+H]^+$. Anal. Calcd. for $C_{26}H_{22}ClN_5OS$: C, 63.99; H, 4.54; N, 14.35; S, 6.57, found: C, 63.90; H, 4.30; N, 14.40; S, 6.51.

*2.1.14. 5-(4-fluorophenyl)-3-phenyl-N'-(4-phenyl-1,3-thiazol-2-yl)-4,5-dihydro-1H -pyrazole-1-carbohydrazide (**3m**).*

Yield, 76%; white solid; m.p. 251-253 ^{0}C. UV-Vis λ_{max} (nm): 289.18, 222.91. IR (cm^{-1}): 3139 (N-H), 2651 (N-H), 1692 (C=O), 1614 (C=N), 1503 (C=N). ^{1}H NMR (DMSO-d_6) δ (ppm): 3.15 (dd, 1H, C<u>H</u>$_a$H, *J* = 5.43 Hz, 18.13 Hz), 3.87 (dd, 1H, CH<u>H</u>$_b$, *J* = 12.19 Hz, 17.98 Hz), 5.49 (dd, 1H, C<u>H</u>$_c$, *J* = 5.46 Hz, 11.86 Hz), 7.20 (s, 1H, C<u>H</u>^{t}), 7.26 (m, 3H, aromatic), 7.40 (m, 2H, aromatic), 7.47 (m, 3H, aromatic), 7.52 (m, 2H, aromatic), 7.80 (d, 2H, aromatic, *J* = 7.42 Hz), 7.88 (m, 2H, aromatic), 9.65 (s, 1H, N<u>H</u>^{2N}), 9.74 (s, 1H, N<u>H</u>^{1N}). ^{13}C NMR (DMSO-d_6) δ (ppm): 41.62, 59.95, 103.13, 125.71, 126.04, 126.82, 127.92, 128.60, 129.03, 130.14, 131.02, 131.42, 131.83, 142.14, 150.12, 152.46, 153.50, 157.96, 173.83. ESI MS: m/z = 458.2 $[M+H]^+$. Anal. Calcd. for $C_{25}H_{20}FN_5OS$: C, 65.63; H, 4.41; N, 15.31; S, 7.01, found: C, 65.60; H, 4.45; N, 15.38; S, 7.10.

*2.1.15. N'-[4-(4-chlorophenyl)-1,3-thiazol-2-yl]-5-(4-fluorophenyl)-3-phenyl-4,5 -dihydro-1H-pyrazole-1-carbohydrazide (**3n**).*

Yield, 76%; yellow solid; m.p. 228-230 ^{0}C. UV-Vis λ_{max} (nm): 290.96, 226.03. IR (cm^{-1}): 3487 (N-H), 3114 (N-H), 1670 (C=O), 1622 (C=N), 1505 (C=N). ^{1}H NMR (DMSO-d_6) δ (ppm): 3.16 (dd, 1H, C<u>H</u>$_a$H, *J* = 5.59 Hz, 18.25 Hz), 3.87 (dd, 1H, CH<u>H</u>$_b$, *J* = 12.12 Hz, 18.46Hz), 5.48 (dd, 1H, C<u>H</u>$_c$, *J* = 5.45 Hz, 11.98 Hz), 7.20 (d, 2H, aromatic, *J* = 8.51 Hz), 7.27 (s, 1H, C<u>H</u>^{t}), 7.45 (m, 5H, aromatic), 7.52 (m, 2H, aromatic), 7.82 (m, 2H, aromatic), 7.88 (m, 2H, aromatic), 9.50 (s, 1H, N<u>H</u>^{2N}), 9.70(s, 1H, N<u>H</u>^{1N}). ^{13}C NMR (DMSO-d_6) δ (ppm): 41.64, 59.99, 103.63, 120.19, 126.81, 127.24, 127.89, 128.54, 128.61, 130.10, 131.08, 131.44, 131.86, 133.36, 142.15, 148.90, 152.40, 153.80, 173.84. ESI MS: m/z = 492.1 $[M+H]^+$. Anal. Calcd. for $C_{25}H_{19}ClFN_5OS$: C, 61.04; H, 3.89; N, 14.24; S, 6.52, found: C, 61.10; H, 3.75; N, 14.31; S, 6.55.

*2.1.16. 5-(4-methylphenyl)-N'-[4-(2-oxo-2H-chromen-3-yl)-1,3-thiazol-2-yl]-3 -phenyl-4,5-dihydro-1H-pyrazole-1-carbohydrazide (**3o**).*

Yield, 72%; white solid; m.p. 211-213 ^{0}C. UV-Vis λ_{max} (nm): 355.90, 291.85. IR (cm^{-1}): 3416 (N-H), 3195 (N-H), 1718 (C=O), 1680 (C=O), 1605 (C=N), 1502 (C=N). ^{1}H NMR (DMSO-d_6) δ (ppm): 2.25 (s, 3H, C<u>H</u>$_3$), 3.11 (dd, 1H, C<u>H</u>$_a$H, *J* = 5.2 Hz, 18.0 Hz), 3.85 (dd, 1H, CH<u>H</u>$_b$, *J* = 12.00 Hz, 18.00 Hz), 5.46 (dd, 1H, C<u>H</u>$_c$, *J* = 5.2Hz, 12.0Hz), 7.12 (m, 4H, aromatic), 7.39 (m, 1H, aromatic), 7.47 (m, 4H, aromatic), 7.62

(m, 1H, aromatic), 7.66 (s, 1H, C<u>H</u>^{t}), 7.87 (m, 3H, aromatic), 8.53 (s, 1H, aromatic), 9.46 (s, 1H, N<u>H</u>^{2N}), 9.70(s, 1H, N<u>H</u>^{1N}). ^{13}C NMR (DMSO-d_6) δ (ppm): 20.61, 41.86, 60.30, 109.76, 115.81, 119.20, 120.55, 124.72, 125.46, 126.81, 128.63, 129.09, 130.02, 131.25, 131.60, 136.31, 138.21, 139.87, 143.94, 152.21, 152.27, 153.78, 158.69, 173.38. ESI MS: m/z = 522.2 $[M+H]^+$. Anal. Calcd. for $C_{29}H_{23}N_5O_3S$: C, 66.78; H, 4.44; N, 13.43; S, 6.15, found: C, 66.74; H, 4.43; N, 13.40; S, 6.10.

2.2. Biology

2.2.1. Anticancer screening

The two cell lines namely, A549 (Human lung carcinoma) and MCF-7 (Breast adenocarcinoma) were procured from NCCS, Pune, India. The cell lines were maintained in 96 wells micro titer plate containing MEM media supplemented with 10% heat-inactivated fetal calf serum (FCS), containing 5% of mixture of gentamicin (10µg), penicillin (100 Units/ ml) and streptomycin (100µg/ml) in presence of 5% CO_2 at 37ºC for 72 h. Briefly, MTT was first prepared as a stock solution of 5 mg/ml in phosphate buffer (PBS, pH 7.2) and was filtered. The cell lines were treated with compounds with different concentrations and the control group contains dimethyl sulfoxide. After 48 h of incubation at 37ºC in a humidified atmosphere of 5% CO_2, a stock solution of MTT was added to each well (20µl, 5mg per ml in sterile PBS) and further incubated for 4 h. 85 ml aliquot of the media was removed from the wells and 50 ml of dimethyl sulfoxide was added to each well and mixed thoroughly with the pipette and incubated at 37^0C. The optical density was measured at 570 nm using LISA-plus to determine the number of viable cells. The percentage of viability was calculated by (AtsX100)/Ac, where Ats is the mean absorption of test compound and Ac is the mean absorption of control. The IC_{50} is the concentration at which, the absorption of treated cells was reduced by 50% with respect to the untreated control.

2.2.2. Antimicrobial activity

In disc diffusion method, the compounds under the test were dissolved in analytically pure dimethyl sulfoxide and with the dilution of 10µg/ml. The test strains were spread on solid agar surface by using sterile swap. The turbidity was adjusted with broth to equal that of 0.5 Mc Farland standards. At the same time, absorbent paper discs were placed on agar surface and impregnated with a known concentration of stain and standard. The plates were inverted and allowed to incubate at 37^0C for about 24 h. The inhibition zone around the disc was calculated edge to edge zone of confluent growth, which was usually, corresponds to the sharpest edge of the zone and to be measured diameter in millimetre.

2.3. Single-crystal X-ray diffraction studies

The X-ray intensity data for single crystals of compounds **3i** and **3k** were collected at a temperature of 296 K on a Rigaku Saturn724 diffractometer using graphite monochromated Mo-Kα radiation. A complete data set was processed using *CrystalClear* [31]. The structure was solved by the direct method and refined by full matrix least squares method on F^2 using *SHELXS* and *SHELXL* programs [32]. All the non-hydrogen atoms were revealed in the first difference Fourier map itself. All the hydrogen atoms were positioned geometrically (C–H = 0.93 Å, N—H = 0.86 Å) and refined using a riding model with U_{iso}(H) = 1.2 U_{eq} and 1.5 U_{eq} (N). After ten cycles of refinement, the final difference Fourier map showed peaks of no chemical significance. The ORTEP and packing diagrams were generated using the software *MERCURY* [33].

2.4. Molecular docking studies

For macromolecular docking studies, chemical structures of the synthesized ligands (**3a-o**), standards like Ciproflaxin and Cisplatin were drawn using Chem Draw Ultra. 3D optimization was performed using Chem Draw 3D Ultra software and stored as .pdb files. Hex docking was carried out by setting suitable parameters. Molecular docking work was performed with the Hex molecular modeling package version 8.0. The ligands were converted to 2D and 3D energy minimized conformations using Hex 3D Ultra 8.0 and the conformation was visualized using Acceryl Discovery Studio 3.1 Client [34].

3. Results and discussion

3.1. Chemistry

The synthetic route for the target thiazole nucleus integrated pyrazoline scaffolds **3a-o** were carried out as outlined in **scheme 1**. The chalcones (**1a-e**) were prepared by utilizing the Claisen-Schmidt reaction. The key intermediate 2-(5-(4-substitutedphenyl)-3-phenyl-4,5-dihydro-1H-pyrazole-1-carbonyl)hydrazinecarbothioamide derivatives (**2a-e)** were synthesized by the coupling of suitable chalcone with carbazide in methanol using potassium carbonate as a base. The resulted *N*-pyrazoline carbohydrazide derivatives were treated with potassium thiocyanate and hydrochloric acid led to the formation of required intermediate **2a-e**. The final thiazole derivatives (**3a-o)** were prepared by treating the suitable intermediate **2a-e** with 2-bromo-1-substitutedethan-1-one in ethanol under reflux condition using sodium acetate.

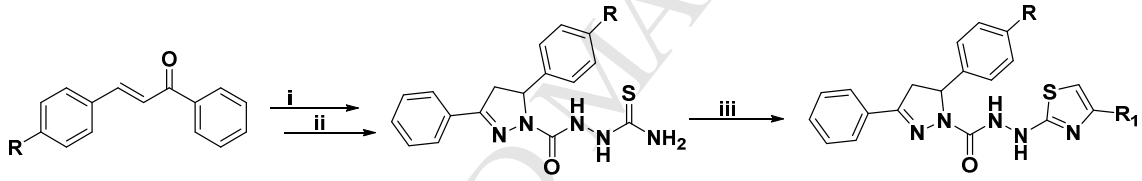

R = Cl(**1a, 2a**), Br(**1b, 2b**), CH_3(**1c**, **2c**), OCH_3(**1d**, **2d**), F(**1e**, **2e**).

Substitution	3a	3b	3c	3d	3e	3f	3g	3h	3i
R	Cl	Br	CH_3	OCH_3	OCH_3	Cl	OCH_3	CH_3	CH_3
R_1	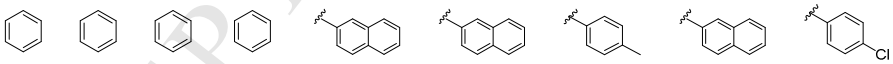								

Substitution	3j	3k	3l	3m	3n	3o
R	Cl	Cl	Cl	F	F	CH_3
R_1	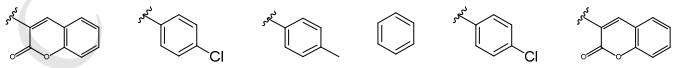					

Reagents and conditions: (i) $NH_2NHCONHNH_2$, K_2CO_3, methanol, 70 ^{0}C, 5 h; (ii) KSCN, HCl, H_2O, 100 ^{0}C, 4 h; (iii) R_1-CO-CH_2-Br, $NaOCH_3$, ethanol, 4h.

Scheme 1. Synthesis of thiazole nucleus integrated with pyrazoline scaffolds **3a-o**.

3.2. Spectral analysis

The UV-Vis spectra of the compounds were characterized by two bands, the first band had the absorption maximum in the range of λ_{max}: 222-237 nm, which was attributed to the intermolecular charge transfer transition owing to the two nitrogen of pyrazoline and

additional phenyl ring at second position of pyrazoline resulting in n - π* transition [35]. The second band had the absorption maximum in the range of λ_{max}: 289-297 nm corresponds to the π-π* transition of C=N-S group [36].

In Infrared spectra, the absorption frequency for the C=N group of the pyrazoline and thiazole ring was observed in the range of 1517-1501 cm^{-1} and 1622-1591 cm^{-1} respectively [37]. The stretching frequency of amide carbonyl group was observed in the range of 1698-1659 cm^{-1} [38]. The absorption bands of amine groups N-H^{2N} and N-H^{1N} (Fig.1) were found in the region from 3304-2651 cm^{-1} and 3487-3139 cm^{-1} respectively.

The ^{1}H and ^{13}C NMR spectra of the compounds were recorded in DMSO-d_6. The two diastereotopic methylene protons (H_a and H_b) and methine proton (H_c) of the pyrazoline ring displayed three doublets of doublets as a ABX pattern with varying coupling constant (*J*) values (Fig. 1). Due to geminal and vicinal coupling, H_a and H_b protons appeared as two doublets of the doublet in the region δ, 3.00 ppm and 3.60 ppm respectively. The chiral proton H_c was resonated in the region δ, 5.50-6.00 ppm as a doublet of doublet, which was due to vicinal coupling with adjacent two protons H_a and H_b. This confirms the presence of pyrazoline ring in the compounds [39]. The thiazole ring has the single proton H^t, which was resonated between δ, 6.78-7.66 ppm [40]. All other aromatic protons were resonated in the region between δ, 7.00-8.00 ppm. The two amine protons H^{1N} and H^{2N} were resonated between δ, 9.00-9.90 ppm.

In ^{13}C NMR spectra, methylene and methine carbon atoms of pyrazoline ring were resonated between δ, 40.30-48.50 ppm and δ, 62.30-67.90 ppm respectively. The signals between δ, 150.10-154.00 ppm and 171.20-175.20 ppm have represented the carbon of C=N group in the pyrazoline and thiazole ring respectively. The aromatic carbons were resonated between δ, 105.38-166.14 ppm. The mass spectra of all synthesized thiazole derivatives were recorded and m/z value of the compounds was matching with the theoretical molecular weight of the compounds. The purities of the compounds were analyzed by elemental analysis.

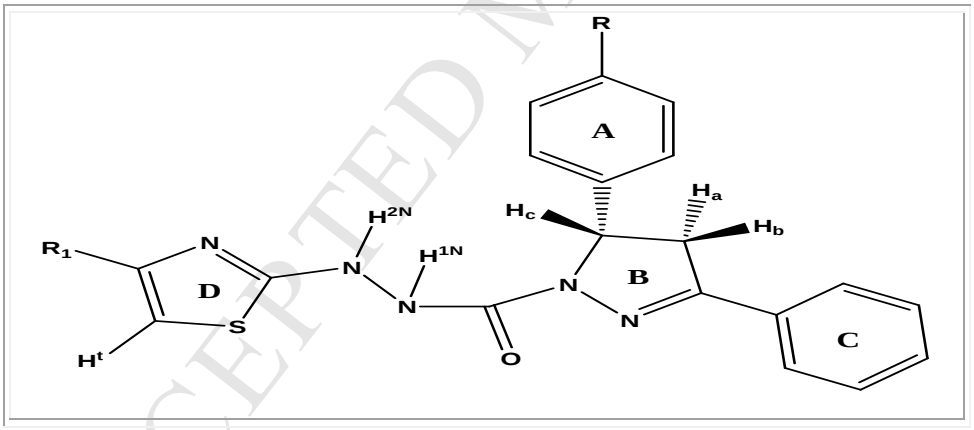

Fig. 1. Labeling of atoms and rings of thiazole nucleus integrated with pyrazoline scaffolds **3a-o**.

3.3. Single crystal X-ray diffraction analysis

The details of the crystal structure and data refinement of the compounds **3i** and **3k** are given in Table 1. The lists of bond lengths and bond angles of the non-hydrogen atoms of the analyzed compounds are given in Table 2 and Table 3 respectively. Figure 2 and 3 represent the ORTEP diagram of the molecules **3i** and **3k** respectively, with thermal ellipsoids drawn at 50% probability.

In the compound **3i**, the thiazole ring (S1/C7/C8/C9/N1) makes a dihedral angle of $83.97(13)^0$, $23.51(13)^0$, $77.77(13)^0$ and $82.27(12)^0$ with pyrazoline ring (C12\C19-C20\N4-N5), 4-chlorophenyl (C1-C6), phenyl (C13-C18) and 4-methylphenyl (C21-C26), respectively. In the compound **3k**, the thiazole ring (S1/C7/C8/C9/N1) makes a dihedral angle of

82.75(14)^0, 22.92(14)^0, 77.02(13)^0 and 81.67(13)^0 with pyrazoline ring (C11\C18-C19\N4-N5), 4-chlorophenyl (C1-C6), phenyl (C12-C17) and terminal 4-chlorophenyl (C20-C25), respectively. Similarly, in the compound **3i**, the pyrazoline ring makes a dihedral angle of 72.56(13)^0, 7.15(13)^0 and 71.46(13)^0 with 4-chlorophenyl, phenyl and 4-methylphenyl respectively. The 4-chlorophenyl moiety makes a dihedral angle of 78.72(13)^0 and 73.83(12)^0 with phenyl and 4-methylphenyl, respectively. The dihedral angle between phenyl and 4-methylphenyl was 69.24(12)^0. In the compound **3k,** pyrazoline ring makes a dihedral angle of 74.41(15)^0, 7.32(14)^0 and 70.94(14)^0 with 4-chlorophenyl, phenyl and terminal 4-chlorophenyl respectively. The 4-chlorophenyl moiety makes a dihedral angle of 80.06(14)^0 and 72.60(14)^0 with phenyl and terminal 4-chlorophenyl, respectively. The dihedral angle between the phenyl and terminal 4-chlorophenyl was 67.80(14)^0.

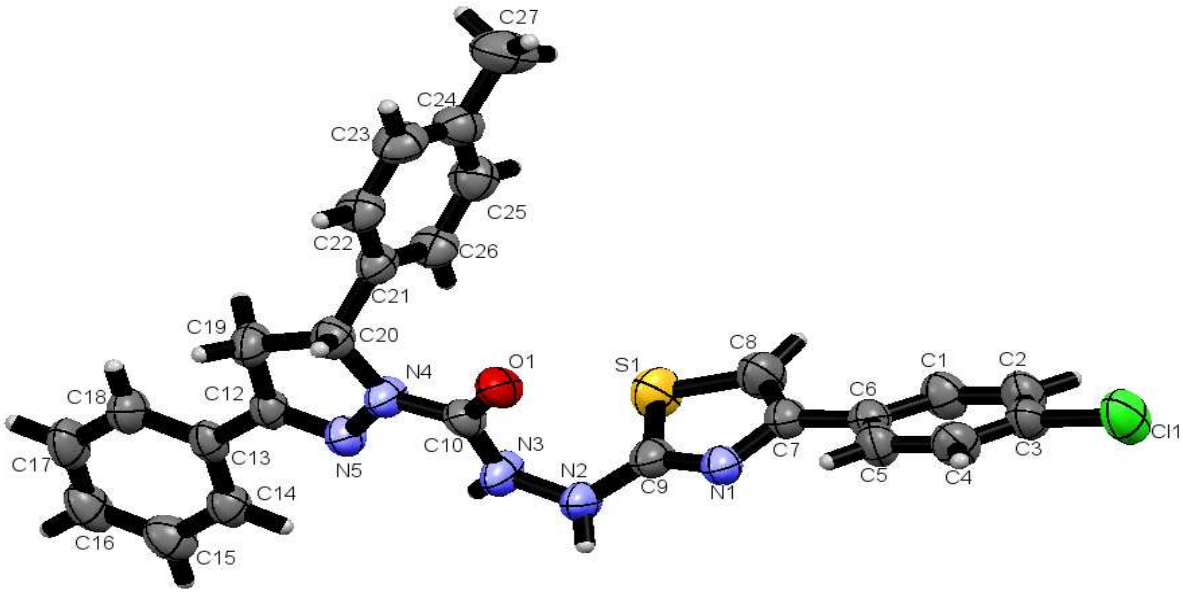

Fig. 2. The molecular structure of the compound **3i**, showing the atomic numbering system. Displacement ellipsoids were drawn at 50% probability.

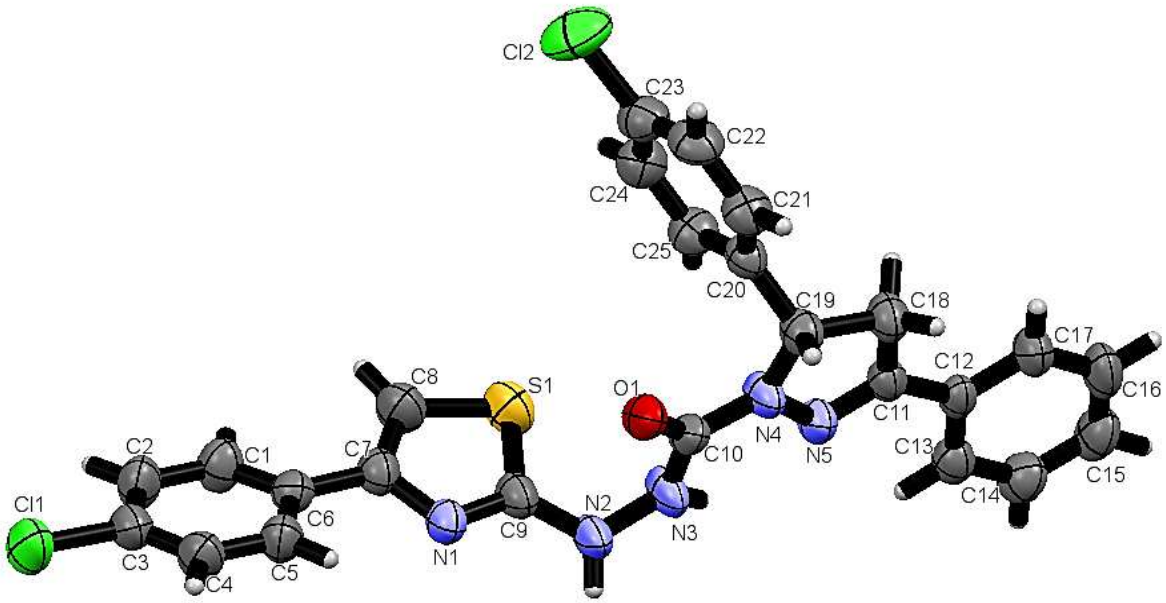

Fig. 3. The molecular structure of the compound **3k**, showing the atomic numbering system. Displacement ellipsoids were drawn at 50% probability.

Table 1
Crystal and structure refinement data of the compounds **3i** and **3k**.

Parameter	**3i**	**3k**
CCDC number	1522900	1522901
Empirical formula	$C_{26}H_{22}ClN_5OS$	$C_{25}H_{19}Cl_2N_5OS$
Formula weight	488.01	508.42
Temperature (K)	293(2)	293(2)
Wavelength (Kα, Å)	0.71075	0.71075
Crystal system, space group	Monoclinic, *P21/n*	Monoclinic, *P21/n*
Unit cell dimensions (Å, º)	*a* = 10.5051(6) *b* = 10.8134(6) *c* = 21.5393(9) β = 98.304(5)	*a* = 10.3950(6) *b* = 10.7085(6) *c* = 21.6339(10) β = 97.991(5)
Volume $Å^3$	2421.1(2)	2384.8(2)
Z, Calculated density (Mg/m^3)	4, 1.339	4, 1.416
Absorption coefficient (mm^{-1})	0.273	0.389
$F_{(000)}$	1016	1048
Crystal size (mm)	0.23 x 0.26 x 0.27	0.20 x 0.20 x 0.20
ø range for data collection (^{0})	2.1 to 52.8	2.1 to 52.8
Limiting indices	$-13\leq h\leq 11$, $-13\leq k\leq 13$, $-26\leq l\leq 26$	$-12\leq h\leq 12$, $-13\leq k\leq 13$, $-27\leq l\leq 27$
Reflections collected / unique[R(int)]	26896/4946 [0.043]	25983 / 4860 [0.046]
Refinement method	Full-matrix least-squares on F^2	Full-matrix least-squares on F^2
Data / restraints / parameters	3494 / 0 / 308	3250 / 0 / 307
R value	0.0530	0.0526
Goodness-of-fit on F^2	1.03	1.05
Largest diff. peak and hole (e. $Å^{-3}$)	0.26 and −0.34	0.26 and −0.32

Table 2
Bond length (Å) of some selected bonds of compounds **3i** and **3k**.

Atoms of **3i**	Bond length	Atoms of **3k**	Bond length
Cl1-C3	1.740(3)	C3-Cl1	1.744(3)
C6-C7	1.470(3)	C7-C6	1.469(3)
N1-C9	1.299(3)	N1-C9	1.294(3)
S1-C9	1.731(2)	S1-C9	1.735(3)
N2-C9	1.369(3)	N2-C9	1.369(3)
N2-N3	1.385(3)	N2-N3	1.385(3)
N5-C12	1.283(3)	N5-C11	1.283(3)
N4-N5	1.385(3)	N4-N5	1.388(3)
N4-C20	1.472(3)	N4-C19	1.461(3)
C20-C21	1.506(3)	C19-C20	1.509(3)

The molecules were connected with intermolecular hydrogen bonds. The packing of the compounds **3i** and **3k** along *a* – axis are given in Figure 4 and 5 respectively. The intermolecular and intramolecular interactions details are given in Table 4. In the compound **3i**, the molecules were connected with intermolecular hydrogen bonds N2—H2...O1, N3----H3...Cl1 and short contacts (C---H... π and C---Cl...π). Also, intramolecular hydrogen bonds N3---H3...N5 and C5----H5....N1 were existed. The short inter contacts C1----H1....Cg4, C5--

-H5...Cg2 and C16---H16...Cg5 were observed. The *Cg*2...*Cg*5 interaction exists with a distance of 3.8773(13)^0, where *Cg*2 and *Cg*5 were N4-N5/C12/C19-C20 and C21-C26, respectively. In the compound **3k**, the molecules were connected with intermolecular hydrogen bonds N2—H2...O1, N3----H3...Cl1 and short contacts (C---H... π and C---Cl...π). Also, intramolecular hydrogen bonds N3---H3...N5 and C5----H5....N1 were existed. The short inter contacts C1----H1....Cg4, C5---H5...Cg2, C15---H15...Cg5 and C16---H16...Cg1 were observed. C23---Cl2...*Cg*1 interaction exists with a distance of 3.6000(15)^0[Cl...Cg1, angle = 101.08 (11)^0, symmetry X,1+Y,Z], where *Cg*1 was S1/C7/C8/C9/N1.

Table 3

Bond angle (°) of some selected bonds of compounds **3i** and **3k**.

Atoms of **3i**	Bond angle	Atoms of **3k**	Bond angle
Cl1-C3-C2	119.9(2)	Cl1-C3-C2	119.5(5)
Cl1-C3-C4	118.8(2)	Cl1-C3-C4	119.1(2)
C5-C6-C7	120.3(2)	C5-C6-C7	120.4(2)
C1-C6-C7	122.1(2)	C1-C6-C7	121.7(7)
C6-C7-N1	118.05(18)	C6-C7-N1	118.3(2)
C7-N1-C9	109.80(18)	C7-N1-C9	110.2(2)
N1-C9-S1	115.94(16)	N1-C9-S1	115.6(2)
C9-S1-C8	88.23(13)	C9-S1-C8	88.13(14)
N1-C9-N2	122.4(2)	N1-C9-N2	122.6(3)
S1-C9-N2	121.54(17)	S1-C9-N2	121.7(2)
C9-N2-N3	117.05(19)	C9-N2-N3	117.4(2)
N2-N3-C10	120.05(19)	N2-N3-C10	120.4(2)
N3-C10-O1	124.0(2)	N3-C10-01	123.7(2)
01-C10-N4	121.5(2)	O1-C10-N4	121.9(2)
C10-N4-N5	120.64(18)	C10-N4-N5	120.5(2)
C10-N4-C20	124.92(18)	C10-N4-C19	124.4(2)
N4-N5-C12	108.13(17)	N4-N5-C11	107.82(19)
N4-C20-C21	112.38(17)	N4-C19-C20	112.6(2)
N5-C12-C13	120.88(19)	N5-C11-C12	120.8(2)
C12-C19-C20	103.54(17)	C11-C18-C19	103.18(18)
C23-C24-C27	117.7(2)	C22-C23-Cl2	119.8(2)
C25-C24-C27	120.5(3)	C24-C23-Cl2	118.8(2)

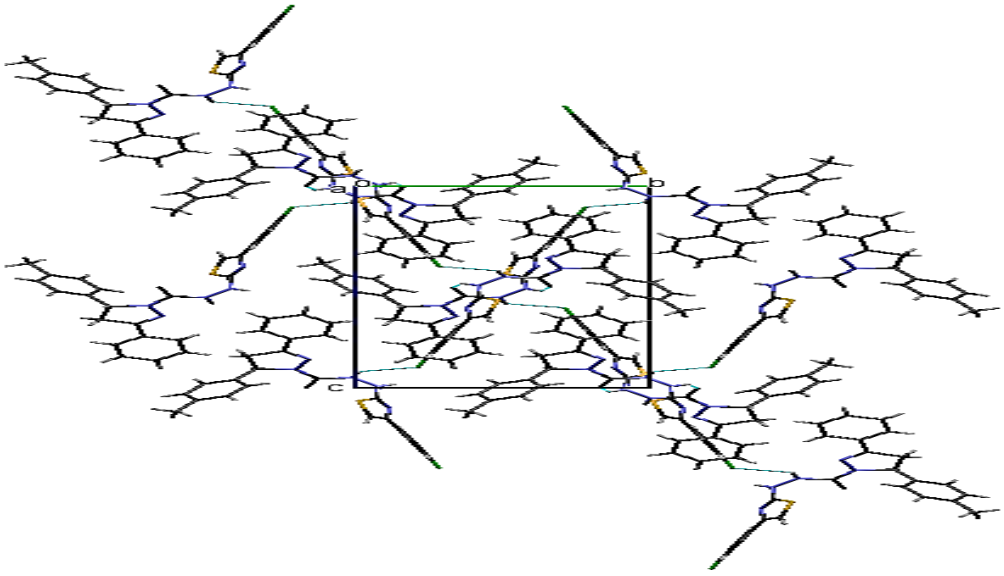

Fig. 4. Packing of the compound **3i** along *a* – axis. Dotted lines indicate hydrogen bonds.

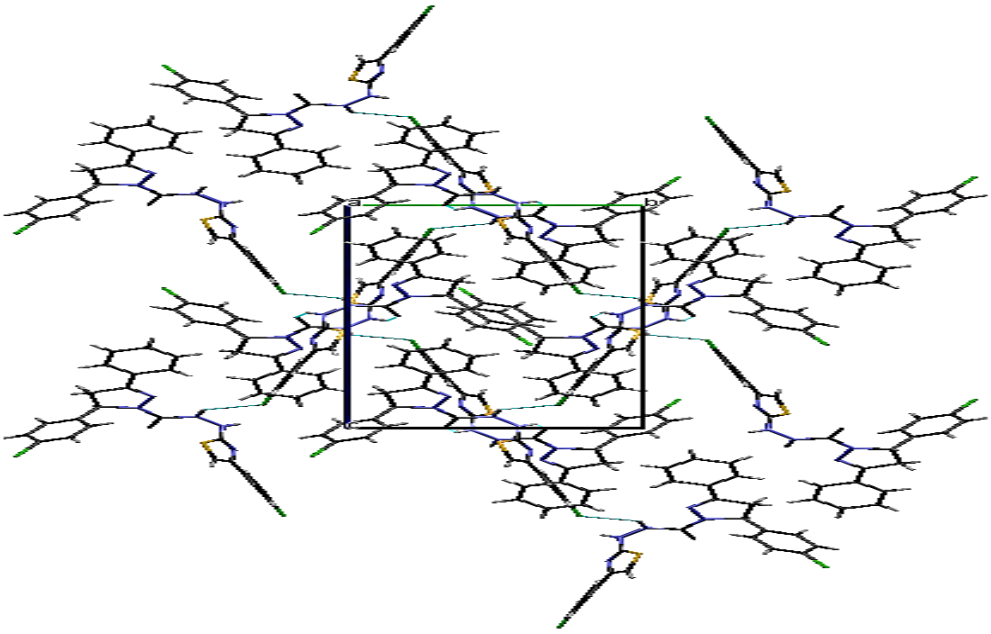

Fig. 5. Packing of the compound **3k** along *a* – axis. Dotted lines indicate hydrogen bonds.

Table 4
Intermolecular and intramolecular interactions of compounds **3i** and **3k**.

Comp.	D---H...A/Cg	D-H (Å)	H...A/*Cg* Å	D....A/*Cg* Å	D---H...A/*Cg* (^{0})
3i	N2---H2...O1^{i}	0.86	2.16	2.829(3)	135
	N3---H3...Cl1^{ii}	0.86	2.59	3.228(2)	132
	N3---H3...N5	0.86	2.26	2.631 (3)	106
	C5---H5...N1	0.93	2.54	2.860 (3)	100
	C1---H1...*Cg*4:C13-C18^{a}	0.93	2.92	3.757(2)	151
	C5---H5...*Cg2*:N4-N5/C12/C19-C20^{b}	0.93	2.93	3.648(2)	135
	C16---H16...*Cg5*:C21-C26^{c}	0.93	2.88	3.729(3)	152
3k	N2---H2...O1^{iii}	0.86	2.14	2.828(3)	136
	N3---H3...Cl1^{iv}	0.86	2.57	3.216(2)	133
	C24---H24...Cl1^{v}	0.93	2.83	3.669(3)	151
	N3---H3...N5	0.86	2.25	2.628(3)	106
	C5---H5...N1	0.93	2.55	2.863(3)	100
	C1---H1...*Cg*4:C13-C18^{d}	0.93	2.87	3.706(3)	150
	C5---H5...*Cg2:*N4-N5/C11/C18-C19^{e}	0.93	2.90	3.630(3)	136
	C15---H15...*Cg5:*C20-C25^{f}	0.93	2.90	3.747(3)	152
	C16---H16...*Cg1:*S1/N1/C7-C9^{g}	0.93	2.99	3.779(3)	143

Symmetry codes:(i) -x,1-y,1-z; (ii) 1/2+x,3/2-y,1/2+z; (iii) 1-x,-y,1-z; (iv) -1/2+x,-1/2-y,-1/2+z; (v) 1/2-x,1/2+y,3/2-z ; (a) 1-X,1-Y,1-Z; (b) -X,1-Y,1-Z; (c) 1/2+X,1/2-Y,1/2+Z; (d) -X,-Y,1-Z; (e) 1-X,-Y,1-Z; (f) -1/2+X,1/2-Y,-1/2+Z; (g) -1/2+X,1/2-Y,-1/2+Z.

3.4. Biological evaluation

3.4.1. Anticancer activity

The compounds **3a-o** were evaluated for their anticancer activity against a panel of two human cancer cell lines namely, A549 (Human lung carcinoma) and MCF-7 (Breast) using the MTT assay [41]. This was based on a colorimetric assay, which takes into account, the ability of a mitochondrial dehydrogenase enzyme from viable cells to cleave the tetrazolium rings of the pale yellow MTT [3-(4,5-dimethylthiazol-2-yl)-2,5-diphenyltetrazoliumbromide] and form dark blue formazan crystals, which was impermeable to cell membranes, thus resulting in its accumulation within healthy cells. The level of formazan created was a reflection of the number of surviving cells and shows a proportionality relationship between them. *In-vitro* activity evaluation was performed under different concentrations (20, 17.5, 15, 12.5, 10. 7.5, 5, 2.5 and 0 mg/mL). Cisplatin was used as a reference cytotoxic compound. The relationship between surviving fraction and drug concentration was plotted to obtain survival curve from which, the response parameter IC_{50} value (concentration required for 50% inhibition of cell viability) was calculated and data is presented in Table 5.

The majority of the synthesized compounds have exhibited promising anticancer activity against the studied cancer cell lines. The compounds, which contain Cl atom at the *para* position of phenyl ring A (**3a**, **3k**) and coumarin group (**3j**) on thiazole ring D, have shown fairly good inhibiting activities over all tested cell lines and displayed IC_{50} values between 5 to 15 µM. By observing the high activity of molecule **3a**, SAR studies were performed by modification of the base compound **3a** to determine, how the substituents of the subunits affect the cell lines inhibitory activities.

As shown in Table 5, structure-activity relationships in compounds **3a-o** demonstrated that, compounds bearing Cl atom at the *para* position of phenyl ring A (Fig.1) have shown better A549 inhibitory activity (compounds **3a**, **3j** and **3k,** the value of IC_{50}, respectively: 12.5, 5.0 and 5.0 µM) than those with F (**3m** and **3n**), Br (**3b**), CH_3 (**3c**, **3h**, **3i** and **3o**) and OCH_3 (**3d**, **3e** and **3g**) substituents at the same position. Basically, the activities were in the order of substitution Cl > F >Br, Cl > CH_3 > OCH_3 on phenyl ring A. The conclusion is, the compound with a stronger the electron withdrawing substituent at the *para* position of phenyl A ring (Cl) had the better A549 and MCF-7 inhibitory activity than that with a relatively weak electron withdrawing substituent (Br) and that of compound with a faintish electron donating substituents at the *para* position of phenyl ring A (CH_3, OCH_3). But the compounds with high electronegative F atom at the *para* position of phenyl ring A (**3m** and **3n**) have shown the considerable less inhibitory activity than the Cl-substituted compounds.

The anticancer activities of the compounds were varied with variation in substitution on ring D. The compounds with naphthalene substitution (**3e, 3f** and **3h**) and *para*-tolyl substitution (**3g** and **3l**) on ring D have shown less inhibitory activity, compared to the compounds with phenyl (**3a**), coumarin (**3j**) and 4-chlorophenyl (**3k**) substitution on the same ring. The order of inhibitory activity on A459 cell lines, based on the substitution of ring D was Coumarin = 4-chlorophenyl > phenyl > 4-methyl phenyl. The compounds with coumarin (**3j**) and 4-chlorophenyl (**3k**) substitution on ring D have shown the two fold more inhibition capacity over A459 cell line, when compared with the standard drug.

3.4.2. Antimicrobial activity

The *in vitro* antimicrobial activity was studied by disc diffusion method [42]. Most of the compounds were active against the bacteria under study (Table 5). The compounds **3a, 3f, 3j, 3k, 3l, 3m** and **3n** have shown the excellent activities against all four tested bacteria and zone of inhibition was closed to that of standard drug Ciprofloxacin. All these compounds have the halogen atom at the *para* position of phenyl ring A. On substitution of electron releasing group like OCH_3 and CH_3 at the *para* position of phenyl ring A, activity was decreased. For example, the compound **3a**, which has the Cl group at the *para* position of

phenyl ring A has shown the zone inhibition of 24 mm, whereas the compound **3d**, with the OCH_3 group at the *para* position of phenyl ring A, has shown the zone inhibition of 18 mm against the bacteria *Staphylococcus aureus.* Even the compounds with halogen atom at the *para* position of phenyl ring A and with different substitution on thiazole ring D, have shown the constant high activity.

Table 5

Anticancer and antimicrobial activity data of thiazole nucleus integrated with pyrazoline scaffolds **3a-o**.

Comp.	IC_{50}(μM)		Zone of inhibition (mm)					
	A549	MCF-7	*S. a*[a]	*B. s*[b]	*E. c*[c]	*P. a*[d]	*C. a*[e]	*A. n*[f]
3a	12.5	10.0	24	26	22	25	20	21
3b	15.0	>20.0	22	25	24	24	21	22
3c	15.0	20.0	19	20	16	18	12	--
3d	>20	>20.0	18	20	19	11	5	--
3e	20	>20.0	20	19	15	13	10	--
3f	7.5	12.5	27	25	28	24	21	5
3g	>20	17.5	15	18	17	15	--	--
3h	15.0	>20.0	16	21	17	16	11	--
3i	12.5	12.5	22	23	22	18	18	12
3j	5.0	10.0	27	24	28	26	27	20
3k	5.0	7.5	22	24	25	26	22	20
3l	10.0	10.0	28	26	25	25	19	18
3m	15.0	15.0	26	22	23	21	21	20
3n	15.0	17.5	25	25	25	24	23	20
3o	>20.0	>20.0	19	15	18	22	16	--
Cisplatin	10	7.5	NA	NA	NA	NA	NA	NA
Ciprofloxacin	NA	NA	27	26	28	25	NA	NA
Fluconazole	NA	NA	NA	NA	NA	NA	27	26

'--' Indicates bacteria were resistant to the compound.
'NA' Indicates not applicable.
a. *S. aureus*, b. *B. subtilis*, c. *E. coli*, d. *P. aeruginosa*, e. *C. albicans*, f. *A. niger.*

The antibacterial activities of thiazole derivatives were depended on the nature of the substitution on phenyl ring A and activity was found in the order of group Cl > Br > F > OCH_3 > CH_3 on phenyl ring A. The compounds with naphthalene (**3f**) and coumarin (**3j**) substitution on ring D have shown the excellent activity.

Most of the molecules have exhibited the antifungal potency against the *Candida albicane* and few molecules were active against the *Aspergillus niger* (Table 5). The compound **3j,** with coumarin group on ring D, has shown the good activity against the *Candida albicane* and the zone of inhibition was equal to that of standard Fluconazole. The compounds with halogen substitution at the *para* position of phenyl ring A (**3a, 3b, 3j, 3k** and **3n**) have shown the comparable good activity than the compounds with CH_3 and OCH_3 groups (**3c, 3d, 3e** and **3g**) at the same position.

3.5. Molecular docking studies

To explore and support the antibacterial and anticancer activity, molecular docking studies of the synthesized compounds **3a-o** were carried out using *E. coli* MurB (PDB code:2MBR) and Jnk1 inhibitor (PDB code:3v3v) enzyme respectively. The docking score can be interpreted as the interaction energy. The selective bonding interaction of the

compounds with the amino acid residue of the enzymes and interaction energy (kcal/mol) are noted in Table 6. More negative E-total value implies that, there exists a strong interaction between drug and receptor and that leads to inhibition of receptor activity.

The interaction of synthesized compounds with the enzymes through different bonds like van der Waals, attractive charge, hydrogen bonds, carbon hydrogen bond, halogen interaction etc. are listed in Table 6. The three-dimensional (3D) interactions of some thiazole compounds with the *E. coli* MurB and Jnk1 inhibitor enzyme are represented in figure 6 and 7 respectively.

Most of the synthesized compounds **3a–o** exhibited a comparable binding interaction energy with the lowest docking score compared to the standard drug Ciprofloxacin (ΔG = -237.66 kcal/mol). The compounds **3f, 3j** and **3l** have shown more least E-total values -323.02, -332.18 and -307.20 kcal/mol respectively. The compounds **3b**, **3c**, **3d**, **3i**, **3k**, **3m** and **3n** have shown the E-total values ranging from -198.67 to -246.71 kcal/mol.

During docking against the Jnk1 inhibitor enzyme, the compounds **3a, 3f, 3i, 3j, 3k** and **3l** have shown minimum binding energy values -114.57, -101.09, -84.39, -78.18, -115.09 and -96.04 kcal/mol respectively. The compounds **3b**, **3c**, **3e**, **3m** and **3n** have also shown the comparable E-total value ranging from -29.22 to -38.52 kcal/mol. The standard drug Cisplatin has the binding energy of -34.15 kcal/mol.

Furthermore, the docking studies of the ligand molecules **3a–o** with *E. coli* MurB and Jnk1 inhibitor enzyme revealed that, all the compounds exhibited bonding with various amino acids in the active pockets. The estimated binding affinity of ligands **3a-o** with the complex hydrogen network with a plethora of amino acids of *E. coli* MurB and Jnk1 inhibitor enzyme includes SER50, PRO111, ILE110, ARG214, ASH51, ILE119, GLN120, ARG327, 1BG159, GLU325 etc, and SER155, HIS149, LYS153, ASP151, SER155, LYS153, HIS149, TYR191, ASP169, ASP207, LEU152, ILE139, ILE167, LYS153, ILE139, LEU152, ILE167, LEU168 etc. respectively. This gives a clue about the importance of hydrogen bond formation for effective enzyme binding. For example, compounds **3j** and **3l** exhibit hydrogen bonds and other interactions (bonds) with SER50, PRO111, ILE110, ARG214, ASN51, LEU218, ALA124, ILE119, SER119, ARG327, GLN120, ARG159 and GLU325, which were present in the active site of *E.coli* MurB enzyme. Thereby potentially inhibiting the bacterial infection causing property of the receptor. The other ligands (compounds) **3a-o** in the series have shown similar interactions. The obtained results may provide a sufficient explanation and good compromise between docking scores and *in vitro* results of the antibacterial and anticancer activity.

Table 6

Results of docking (binding energy) and bonding interaction of thiazole nucleus integrated with pyrazoline scaffolds **3a-o**.

Comp.	*E.Coli* MurB		JnK1 Inhibitor	
	-ΔG (kcal/ mol)	Bonding interaction	-ΔG (kcal/ mol)	Bonding interaction
3a	240.63	SER50:PRO111:ILE110: ARG214:ASH51: ILE119: GLN120:ARG327:IBG159: GLU:325	114.57	SER155:LYS153:ASP:154: ILE157:ILE167:ILE139: PHE170:ASP207:ASN156: HSP169:LEU152:LEU142: SER210:LEU168:TRP209: ARG150:LYS55:GLY35
3b	205.12	SER50:ARG327:GLU325: GLN120:ILE110:ILE119: PRO111	29.22	SER155:HIS149:LYS153: ASP151:TYR191:ASP169: ASP207:LEU152:ILE139: ILE167:LYS153:LEU168
3c	198.67	ILE119:ARG327:TYR158: ASN51:GLN120:ARG159: GLU325:PRO111:ARG214: ILE110:SER50	31.70	ILE139:ILE167:SER210: LEU152:LEU148:HIS149: ASP151:ASN156:ASP169: LEU168:LYS153:SER155
3d	230.56	SER50:ARG327:GLU325: TYR158:ARG159:ILE110: ILE119:PRO111	19.41	SER155:LYS153:VAL206: ASP207:ASP151:ASP169: LEU152:ILE139:ILE167: LEU168
3e	232.95	SER50:ARG327:GLU325: ILE110:PRO111:ILE119: ILE110:ALA124:ARG214: LEU218:ILE110:PRO111	39.96	SER155:LYS153:HIS149: VAL206:ASP207:ASP151: ASP169:LEU168:ILE139: ILE167: ILE13: LEU152
3f	323.02	ARG327:ALA124:LEU218: ILE110:LIE119:ARG214: GLN120:ARG159:ASN51 :SER50	101.09	ASP207:ILE139:SER210: LEU152:LEU142:HIS149: ASP151:LYS153:ASN156: ASP169:LEU168:SER155: ILE167:VAL211:TRP209
3g	208.81	TY158:GLU325:ARG159: SER50:ARG214:ALA124: LEU218:ILE110:PRO111: GLN120:ASN51:ARG327: ILE119	25.31	LEU168:LEU142:ASP151: LYS153:ASN156:ASP169: LYS55:ILE139:ILE167: LEU152:SER210:VAL211: SER155:ASP207:TRP209: VAL206
3h	220.54	GLU325:ARG327:LEU218: ALA124:ILE119:ARG214: GLN120:ARG159:ASN51: SAR50:PRO111:ILE110	18.89	VAL206:TRP209:SAR210: ILE167:ILE139:LEU152: LEU142:LYS55:ASP169: ASN156:ASP154:HIS149: ASP207:SER155:LYS153: LEU168
3i	213.0	GLU325:ARG159:SER50: LEU218:ALA124:GLN120: TYR158:ASN51:ARG327: ILE119:PRO111:ILE110: ARG214	84.39	LEU142:HIS149:LYS153: SER155:ASP151:LEU162: ASN156:LEU168:ILE139: ILE167:ASP207:SER210: ASP169:TRP209:GLU173: LYS55
3j	332.18	GLU325:SER50:ARG159: ASN51:GLN120:ARG214: PRO111:ARG327:ILE119: ILE110:LEU218:ALA124	78.18	SER155:ASP207:HIS149: LEU142:ASP151:LYS153: LEU168:GLU73:ASP169: ASN156:LYS55:LEU152: SER210:ILE139:ILE167: VAL211:TRP209
3k	246.71	GLU325:ARG158:SER50:	115.09	LEU142:HIS149:LEU168:

		ILE122:GLN120:TYR158: ASN51:ARG327:ILE119: PRO111:ILE110:ARG214: SER116:ALA124		LYS153:ASP151:ASN156: LEU152:ILE139:ILE167: ASP169:ASP207:SAR210: VAL11I:LYS55
3l	307.20	SER50:PRO111:ILE110: ARG214:ASN51:LEU218: ALA124:ILE119:SER119: ARG327:GLN120:ARG159: GLU325	96.04	SER155:LEU168:LYS153: ASP151:ILE167:ASP169: ASN156:LEU152:HS149: LYS55:LEU142:TRP209: SER210:ILE139:ASP207
3m	236.65	SER50:SER116:ARG327: GLU325:ILE119:GLN120: ILE110:PRO111	30.38	SER155:SP151:LYS153: TYR191:VAL206:TRP209: SER210:ASP169:ASP207: LEU168:LEU152:ILE139: ILE167:ILE139:LEU152
3n	227.31	SER116:SER50:ARG327: GLU325:GLN120:ALA124: ILE110:ARG214:LEU218: ILE119	38.52	LYS153:HIS149:ASN156: TRP209:TYR191:SER210: LEU152:ASP151:SER155: GLU73:VAL206:ASP169: ASP207:ILE139:ILE167: LYS55:LEU168
3o	217.62	SER50:ARG327:GLU325: PRO111:ALA124:ARG214: LEU218: ILE110:PRO111	24.08	SAR155:LYS153:LEU168: ASP151:HIS149:ASP207: LEU142:LEU152:LYS55: ASN156:ASP169:SER210: ILE139:ILE167:TRP209
Ciprofloxacin	237.66	GLU325:ARG158:SER50: ILE122:GLN120:TYR158: ASN51:ARG327:ILE119: PRO111:ILE110:ARG214: SER116:ALA124	--	--
Cisplatin	--	--	34.15	SER155:SP151:LYS153: TYR191:VAL206:TRP209: SER210:ASP169:ASP207: LEU168:LEU152:ILE139: ILE167:ILE139:LEU152

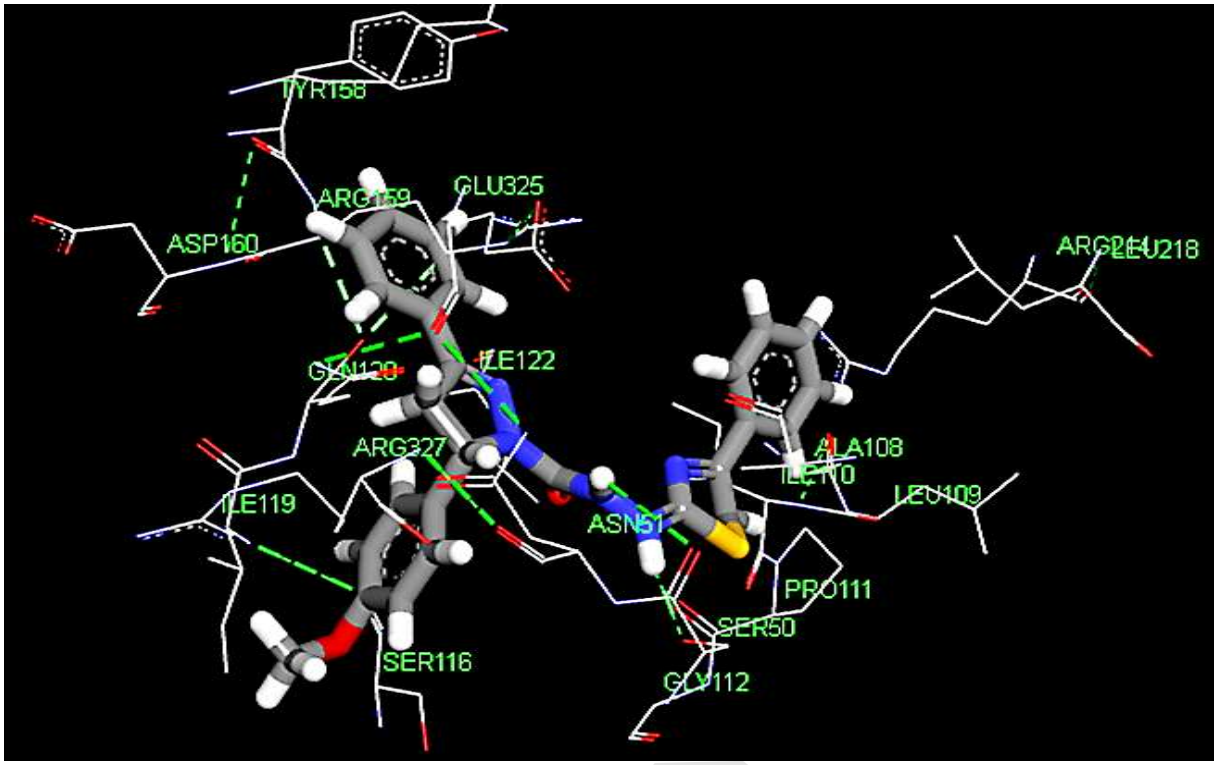

3d

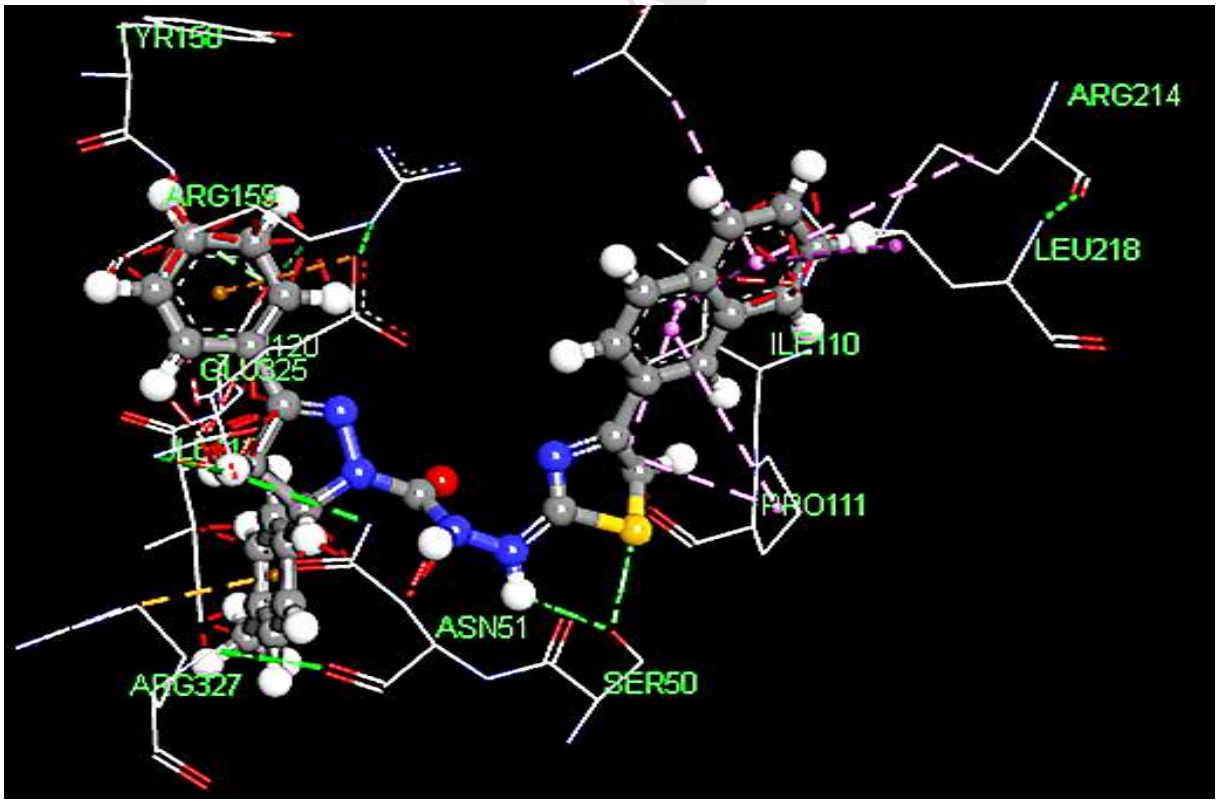

3h

Fig. 6. Three-dimensional interactions of compounds with the active site amino acids of *E. coli* MurB enzyme.

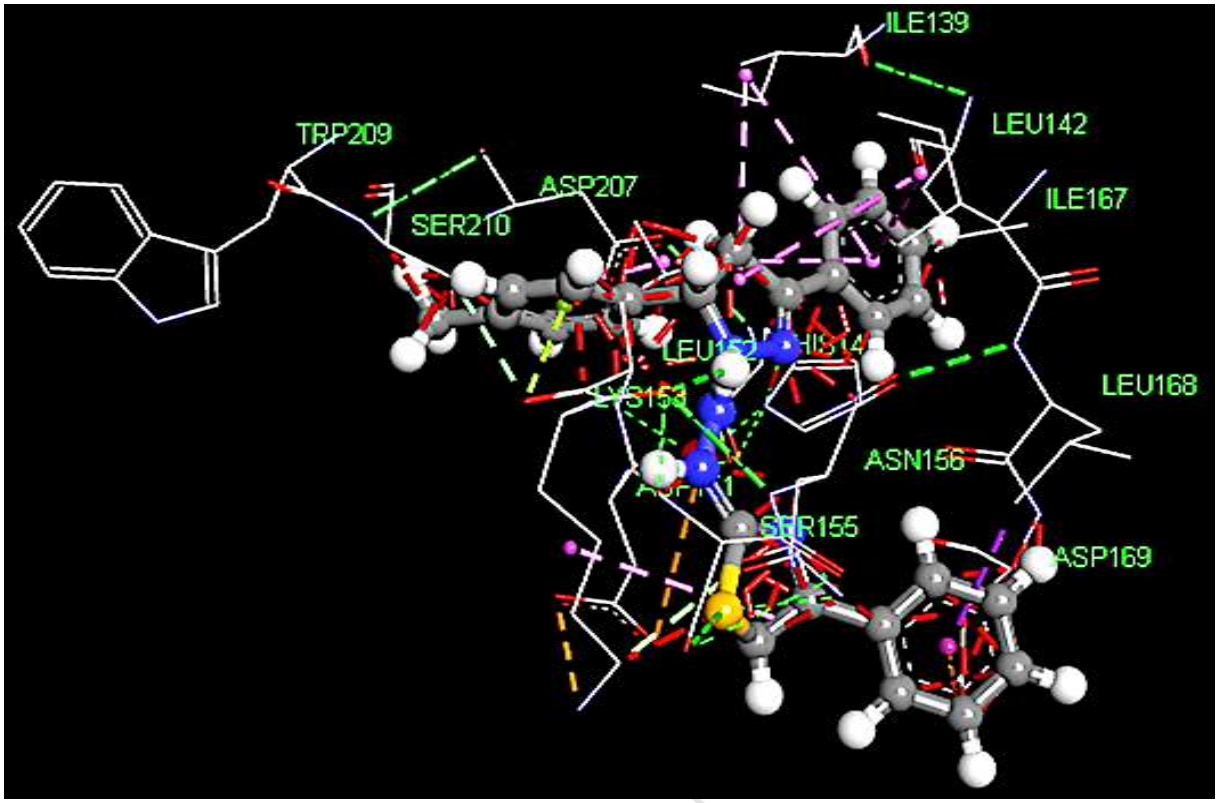

3c

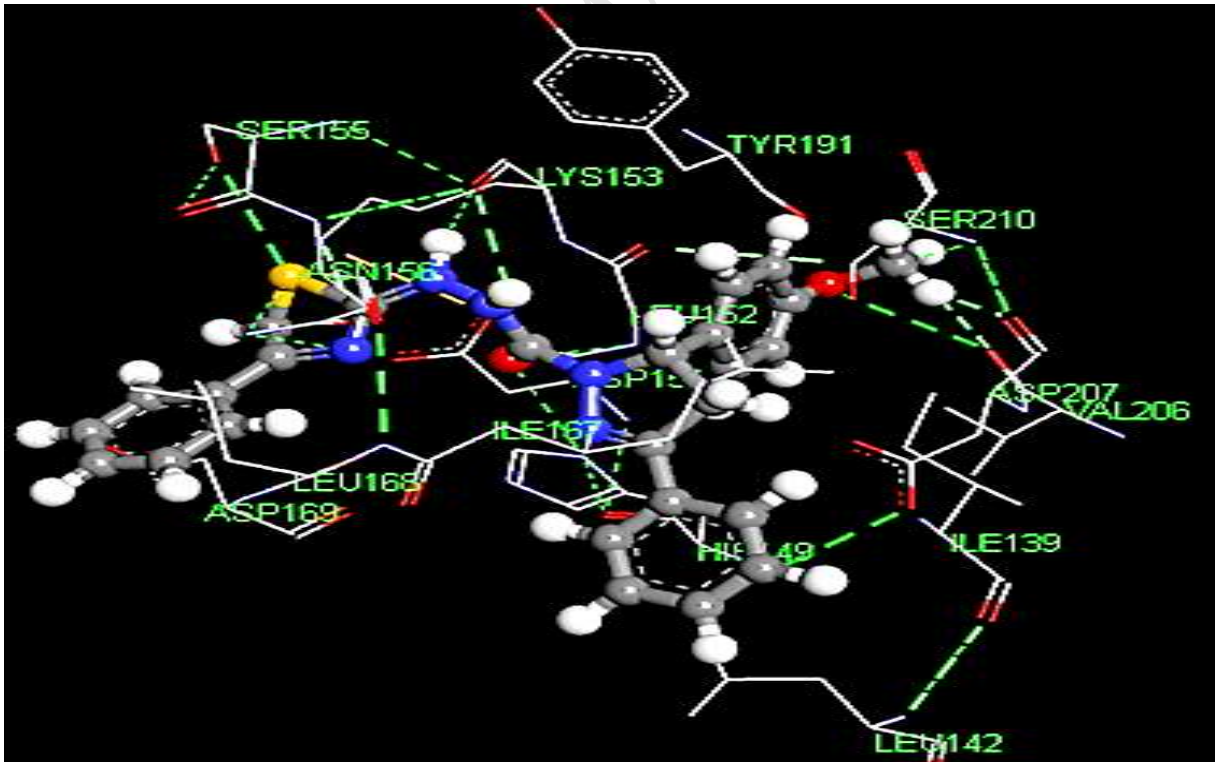

3d

Fig. 7. Three-dimensional interactions of compounds with the active site amino acids of Jnk1 inhibitor.

4. Conclusion

A new series of thiazole nucleus integrated with pyrazoline scaffolds bearing different substituents were synthesized in appreciable yields. The spectroscopic techniques namely, UV-Vis, FTIR, ^{1}H NMR, ^{13}C NMR and mass spectra were used to arrive at the structural characterization. The single crystal X-ray diffraction studies on molecules **3i** and **3k** revealed that, the molecules were connected with the intermolecular hydrogen bonds N2—H2...O1. N3----H3...Cl1 and N2—H2...O1. N3----H3...Cl1 respectively, also intramolecular hydrogen bonds and shorts contacts. The newly synthesized analogues were evaluated for their *in vitro* anticancer and antimicrobial activity. The compounds **3a, 3j** and **3k** having the Cl atom at the *para* position of phenyl ring A have shown the IC_{50} value better than the standard drug against two human cancer cell lines namely A549 and MCF-7. The compounds having halogen atoms at the *para* position of phenyl ring A, like compounds **3a, 3f, 3j, 3k, 3l, 3m** and **3n** have shown the best antimicrobial activity over studied microorganism. The SAR study was supported by the molecular docking study against *E. coli* MurB and Jnk1 inhibitor enzymes. The obtained binding interaction and energy had a good correlation with the biological potency of the molecules.

Acknowledgements

The authors are thankful to Sigma-Aldrich Chemical Pvt. Ltd. Bengaluru, India, for providing necessary laboratory facilities for the research work, funding and valuable support. Authors are also thankful to the DST-PURSE Lab, Mangalore University for single crystal X-ray diffraction data.

References

1. American Cancer Society, Cancer Facts and Figures (2015).
2. A.R. Ali, E.R. El-Bendary, M.A. Ghaly, I.A. Shehata, Synthesis, *in vitro* anticancer evaluation and *in silico* studies of novel imidazo[2,1-b] thiazole derivatives bearing pyrazole moieties, Eur. J. Med. Chem. 75 (2014) 492-500.
3. S. Koppireddi, D.R. Kumari Chilaka, S. Avula, J.R. Komsani, S. Kotamraju, R. Yadla, Synthesis and anticancer evaluation of 3-aryl-6-phenylimidazo[2,1-b]thiazoles, Bioorg. Med. Chem. Lett. 24 (2014) 5428-5431.
4. R. Romagnoli, P.G Baraldi, M.K. Salvador, M.E. Camacho, D. Preti, M.A. Tabrizi, M. Bassetto, A. Brancale, E. Hamel, R. Bortolozzi, G. Basso, G. Viola, Synthesis and biological evaluation of 2-substituted-4-(30,40,50-trimethoxyphenyl)-5-aryl thiazoles as anticancer agents, Bioorg. Med. Chem. 20 (2012) 7083-7094.
5. M. Schnürch, B. Waldner, K. Hilber, M.D. Mihovilovic, Synthesis of 5-arylated N-arylthiazole-2-amines as potential skeletal muscle cell differentiation promoters, Bioorg. Med. Chem. Lett. 21 (2011) 2149-2154.
6. K.D. Hargrave, F.K. Hess, J.T. Oliver, N-(4-Substituted-thiazolyl)oxamic acid derivatives, new series of potent, orally active antiallergy agents, J. Med. Chem. 26 (1983) 1158-1163.
7. W.C. Patt, H.W. Hamilton, M.D. Taylor, M.J. Ryan, D.G. Jr. Taylor, C.J.C. Connolly, A.M. Doherty, S.R. Klutchko, I. Sircar, Structure activity relationships of a series of 2-amino-4-thiazole containing renin inhibitors, J. Med. Chem. 35 (1992) 2562-2572.
8. R.N. Sharma, F.P. Xavier, K.K. Vasu, S.C. Chaturvedi, S.S. Pancholi, Synthesis of 4-benzyl-1,3-thiazole derivatives as potential anti-inflammatory agents: an analogue based drug design approach, J. Enz. Inhib. Med. Chem. 24 (2009) 890-897.
9. J.C. Jaen, L.D. Wise, B.W. Caprathe, H. Tecle, S. Bergmeier, C.C. Humblet, T.G. Heffner, L.T. Meltzner, T.A. Pugsley, 4-(1,2,5,6-tetrahydro-1-alkyl-3-pyridinyl)-2-

thiazolamines: a novel class of compounds with central dopamine agonist properties, J. Med. Chem. 33 (1990) 311-317.
10. K. Tsuji, H. Ishikawa, Synthesis and anti-pseudomonal activity of new 2-isocephems with a dihydroxypyridone moiety at C-7, Bioorg. Med. Chem. Lett. 4 (1994) 1601-1606.
11. F.W. Bell, A.S. Cantrell, M. Hogberg, S.R. Jaskunas, N.G. Johansson, C.L. Jordon, M.D. Kinnick, P. Lind, J.M. Jr. Morin, R. Noreen, B. Oberg, J.A. Palkowitz, C.A. Parrish, P. Pranc, C. Sahlberg, R.J. Ternansky, R.T. Vasileff, L. Vrang, S.J. West, H. Zhang, X.X. Zhou, Phenethylthiazolethiourea (PETT) compounds, a new class of HIV-1 reverse transcriptase inhibitors. 1. Synthesis and basic structure activity relationship studies of PETT analogs, J. Med. Chem. 38 (1995) 4929-4936.
12. N. Ergenc, G. Capan, N.S. Gunay, S. Ozkirimli, M. Gungor, S. Ozbey, E. Kendi, Synthesis and hypnotic activity of new 4-thiazolidinone and 2-thioxo- 4,5-imidazolidinedione derivatives, Arch. Pharm. 332 (1999) 343-347.
13. A. Tabbi, Z.A Kaplancikli, D. Tebbani, L. Yurttas, Z. Canturk, O. Atli, M. Baysal, G. Turan-zitouni, Synthesis of novel thiazolylpyrazoline derivatives and evaluation of their antimicrobial activities and cytotoxicities, Turk. J. Chem. 40 (2016) 641-654.
14. N.C. Desai, V.V. Joshi, K.M. Rajpara, Synthesis of new quinoline-2-pyrazoline-based thiazolinone deriavitves as potential antimicrobial agents, Med. Chem. Res. 22 (2013) 3663-3674.
15. S. Bondock, W. Fadaly, M.A. Metwally, Synthesis and antimicrobial activity of some new thiazole, thiaphene and pyrazole derivatives containing benzothiazole moiety, Eur. J. Med. Chem. 45 (2010) 3692-3701.
16. E.M. Sharshira and N.M.M. Hamada, Synthesis, characterization and antimicrobial activities of some thiazole derivatives, Am. J. Org. Chem. 2 (2012) 69-73.
17. D. Mengin-Lecreulx, B. Flouret, J. van Heijenoort, Cytoplasmin steps of peptidoglycan synthesis in Escherichia coli, J. Bacteriol. 151 (1982) 1109-1017.
18. Y. Yang, A. Severin, R. chopra, G. Krishnamurthy, G. Singh, W. Hu, D. Keeney, K. Svenson, P.J. Petersen, P. Labthavikul, D.M. Shlaes, B.A. Rasmussen, A.A. Failli, J.S. Shumsky, K.M.K. Kutterer, A. Gilbert, T.S. Mansour, 3,5-Dioxopyrazolidines, novel inhibitors of UDP-N-acetylenolpyruvylglucosamine reductase (MurB) with activity against gram-positive bacteria, J. Antimicrob. Chemother. 50 (2006) 556-564.
19. M.B. Sapkal, H.D. More, One pot three component syntheis of Pyrimidine-5-carbonitrile derivatives in water using *P*-dodecylbenzenesulfonic acid as catalyast and evaluation of *in vitro* anti-inflammatory and anthelmintic activities, Der Pharma Chemica. 7 (2015) 167-173.
20. C. Bubici, S. Papa, JNK signalling in cancer: in need of new, smarter therapeutic targets, Br. J. Pharmacol. 171 (2014) 24-37.
21. E. Lee, K.W. Jeong, A. Shin, Y. Kim, Anti-inflammatory activity of 3,6,3′-trihydroxyflavone in mouse macrophages, *In vitro*, Bull. Korean Chem. Soc. 35 (2014) 3169-3174.
22. D.-W. Fu, H.-L. Cai, Y. Liu, Q. Ye, W. Zhang, Y. Zhang, X.-Y. Chen, G. Giovannetti, M. Capone, J. Li, R.-G. Xiong, Diisopropylammonium bromide is a high-temperature molecular ferroelectric crystal, science, 339 (2013) 425-428.
23. D.-W. Fu, W. Zhang, H.-L. Cai, Y. Zhang, J.-Z. Ge, R.-G. Xiong, S.D. Huang, Supramolecular bola-like ferroelectric: 4-methoxyanilinium tetrafluoroborate-18-crown-6, J. Am. Chem. Soc. 133 (2011) 12780-12786.
24. D.-W. Fu, W. Zhang, H.-L. Cai, J.-Z. Ge, Y. Zhang, R.-G. Xiong, Diisopropylammonium chloride: A ferroelectric organic salt with a high phase transition temperature and practical utilization level of spontaneous polarization, Adv. Mater. 23 (2011) 5658-5662.

25. D.-W. Fu, W. Zhang, H.-L. Cai, Y. Zhang, J.-Z. Ge, R.-G. Xiong, S.D. Huang, T. Nakamura, A multiferroic perdeutero metal-organic frame work, Angew. Chem. Int. Ed. 50 (2011) 11947-11951.
26. D.-W. Fu, H.-L Cai, S.-H. Li, Q. Ye, L. Zhou, W. Zhang, Y. Zhang, F. Deng, R.-G. Xiong, 4-Methoxyanilinium perrhenate 18-crown-6: A new ferroelectric with order originating in swing like motion slowing down, Phys. Rev. Lett. 110 (2013) 257601.
27. W.-Y. Zhang, Q. Ye, D.-W. Fu, R.-G. Xiong, Optoelectronic duple bistable switches: A bulk molecular single crystal and unidirectional ultraflexible thin film based on imidazolium fluorochromate, Adv. Funct. Mater. 27 (2017) 1603945-1603953.
28. B.P. Bandgar, L.K. Adsl, H.V. Chavan, S.S. Jalde, S.N. Shringare, R. Shaikh, R.J. Meshram, R.N. Gacche, V. Masand, Synthesis, biological evaluation and docking studies of 3-(substituted)-1-aryl-5-(9-methyl-3-carbazole)-1*H*-2-pyrazolines as potent anti-inflammatory and antioxidant agents, Bioorg. Med. Chem. Lett. 22 (2012) 5839-5844.
29. A.A. Biligin, E. Palaska, R. Sunal, Studies on the synthesis and antidepressant activity of some 1-thiocarbamoyl-3,5-diphenyl-2-pyrazolines, Arzneimittelforschung, 43 (1993) 1041-1044.
30. N.C. Desai, H.V. Vaghani, K.M. Rapara, V.V. Joshi, H.M. Satodiya, Novel approach for synthesis of potent antimicrobial hybrid molecules containing pyrimidine-based imidazole scaffolds, Med. Chem. Res. 23 (2014) 4395-4403.
31. Rigaku, CrystalClear-SM Expert and crystalstructure, Rigaku Corporation, Tokyo, Japan (2011).
32. (a) G.M. Sheldrick, A short history of *SHELX*, Acta Cryst. A64 (2008) 112-122. (b) G.M. Sheldrick, Crystal structure refinement with SHELXL, Acta Cryst. C71 (2015) 3-8.
33. C.F Macrae, I.J Bruno, J.A. Chisholm, P.R. Edgington, P. McCabe, E. Pidcock, L. Rodriguez-Monge, R. Taylor, J. van de Streek, P.A. Wood, Mercury CSD 2.0 – new features for the visualization and investigation of crystal structures, J. Appl. Cryst. 41 (2008) 466-470.
34. M. Bhat, G.K. Nagaraja, R. Kayarmar, S.K. Peethamber, M.R. Shafeeulla, Design, synthesis and characterization of new 1,2,3-triazolyl pyrazole derivatives as potential antimicrobial agents *via* a Vilsmeier-Haack reaction approach, RSC Adv. 6 (2016) 59375-59388.
35. A.R. Bhat, F. Athar, A. Azam, Bis-pyrazolines: synthesis, characterization and antiamoebic activity as inhibitors of growth of *Entamoeba histolytica*, Eur. J. Med. Chem. 44 (2009) 426-431.
36. Z.A. Naser Al-Shamkhani, H.A. Al-Hazam, Microwave assisted synthesis, characterizations and antibacterial activity of some of thiazole derivatives, Res. J. Pharm., Biol. Chem. Sci. 6 (2015) 718-725.
37. B.H. Stuart, Infrared spectroscopy: Fundamentals and applications, Wiley (2014).
38. A. Taurins, J.G.E. Fenyes, R.N. Jones, Thiazoles: iii. Infrared spectra of methylthiazoles, Can. J. Chem. 35 (1957) 423-427.
39. A. Hassner, M.J. Michelson, NMR spectra and stereoisomerism in pyrazolines, J. Org. Chem. 27 (1962) 3974-3976.
40. D. Azarifar, M. Shaebanzadeh, Synthesis and characterization of new 3,5-dinaphthyl substituted 2-pyrazolines and study of their antimicrobial activity, Molecules, 7 (2002) 885-895.
41. T. Mossman, Rapid colorimetric assay for cellular growth and survival: application to proliferation and cytotoxicity assays, J. Immunol. Methods, 65 (1983) 55-63.
42. H.D. Isenberg, Clinical microbiology procedures handbook, American society for Microbiology, Washington D. C. 1992.

Synthesis, structure characterization, *in vitro* and *in silico* biological evaluation of a new series of thiazole nucleus integrated with pyrazoline scaffolds

Rajitha Sadashiva[a], Damodara Naral[b], Jyothi Kudva[c*], S. Madan Kumar[d], Byrappa K[e], Mohammed Shafeeulla R[f], Manjunatha Kumsi[g].

[a]Sigma-Aldrich Chemical Pvt. Ltd., Bommasandra-Jigani link Road, Bengaluru, 560100, INDIA.
[b]Department of Chemistry, Canara Engineering College, Benjanapadavu, Mangaluru, 574219, INDIA.
[c*]Department of Chemistry, St Joseph Engineering College, Vamanjoor, Mangaluru, 575005, INDIA.
[d]DST-PURSE Lab., Mangalagangotri, Mangalore University, Mangaluru, 574199, INDIA.
[e]Department of Materials Science, Mangalagangotri, Mangalore University, Mangaluru, 574199, INDIA.
[f]Department of Chemistry, Sahyadri Science College, Shimoga, 577 201, INDIA.
[g]Department of Chemistry, Nagarjuna College of Engineering and Technology, Bengalure, 562164, INDIA.

Highlights:

- 2,4-disubstituted-1,3-thiazole linked with pyrazoline scaffolds were synthesized and characterized by spectroscopic techniques.
- Anticancer screening done against A549 and MCF-7 human cancer cell lines.
- Docked against *E. coli* MurB (PDB code: 2MBR) and Jnk1 inhibitor (PDB code: 3v3v) enzymes.